Supporting Information

A π-Conjugated System with Flexibility and Rigidity that Shows Environment-Dependent RGB Luminescence

Chunxue Yuan,[†] Shohei Saito,*[,†,‡] Cristopher Camacho,[†] Stephan Irle,*[,†,¶] Ichiro Hisaki,[§] and Shigehiro Yamaguchi*[,†,¶]

[†]*Department of Chemistry, Graduate School of Science, Nagoya University, Furo, Chikusa, Nagoya 464-8602, Japan.*

[‡]*PRESTO, Japan Science and Technology Agency (JST), Furo, Chikusa, Nagoya 464-8602, Japan.*

[¶]*Institute of Transformative Bio-Molecules (WPI-ITbM), Nagoya University, Nagoya 464-8602, Japan.*

[§]*Department of Material and Life Science, Graduate School of Engineering, Osaka University, Yamadaoka, Suita, Osaka 565-0871, Japan.*

**e-mail: s_saito@chem.nagoya-u.ac.jp; sirle@chem.nagoya-u.ac.jp; yamaguchi@chem.nagoya-u.ac.jp*

Contents

1. Experimental details

General. Melting points (mp) were measured by a Stanford Research System MPA100 OptiMelt instrument. ^{1}H and ^{13}C NMR spectra were recorded with a JEOL AL-400 (400 MHz for ^{1}H and 100 MHz for ^{13}C) spectrometer. The chemical shifts are reported in δ ppm with reference to residual protons and carbons of $CDCl_3$ (7.26 ppm in ^{1}H NMR and 77.16 ppm in ^{13}C NMR), DMSO-d_6 (2.50 ppm in ^{1}H NMR and 39.52 ppm in ^{13}C NMR) and *o*-dichlorobenzene-d_4 (6.94 ppm in ^{1}H NMR). Mass spectra were measured with a Bruker Daltonics micrOTOF-focus using the APCI-TOF method in the positive-ion mode in toluene. Thin layer chromatography (TLC) was performed on glass plates coated with 0.25 mm thickness of Silica Gel 60F-254 (Merck). Column chromatography was performed using neutral silica gel PSQ100B (Fuji Silysia Chemical). UV-vis absorption spectra were recorded on a Shimadzu UV-3150 spectrometer. Fluorescence spectra of a solution and a poly(methyl methacrylate (PMMA) film of samples were recorded on a Hitachi F-4500 spectrometer. Absolute fluorescence quantum yields (Φ) were determined with a Hamamatsu C9920-02 calibrated integrating sphere. Solid-state diffusion reflectance spectra were recorded on a JASCO V-570 spectrometer. The samples were measured in a CH_2Cl_2 solution (2×10^{-6} M), in the crystalline state, and in a sample-doped PMMA film. The PMMA film was prepared on the surface of a quartz cell by casting a $CHCl_3$ solution (10 mL) of the sample (5 mg) and PMMA (500 mg, typical M_w = 15000, Aldrich). Fluorescence lifetimes were measured with a Hamamatsu picosecond fluorescence measurement system C4780. All reactions were performed under a nitrogen atmosphere, unless stated otherwise. Commercially available solvents and reagents were used without further purification except triethylamine, which was distilled over CaH_2. Dry THF and CH_2Cl_2 were purchased from Kanto Chemicals. 2,3,6,7-Tetrakis(methoxycarbonyl)-9,10-dihydro-9,10-ethenoanthracene (**3**) was prepared according to the literature.[S1]

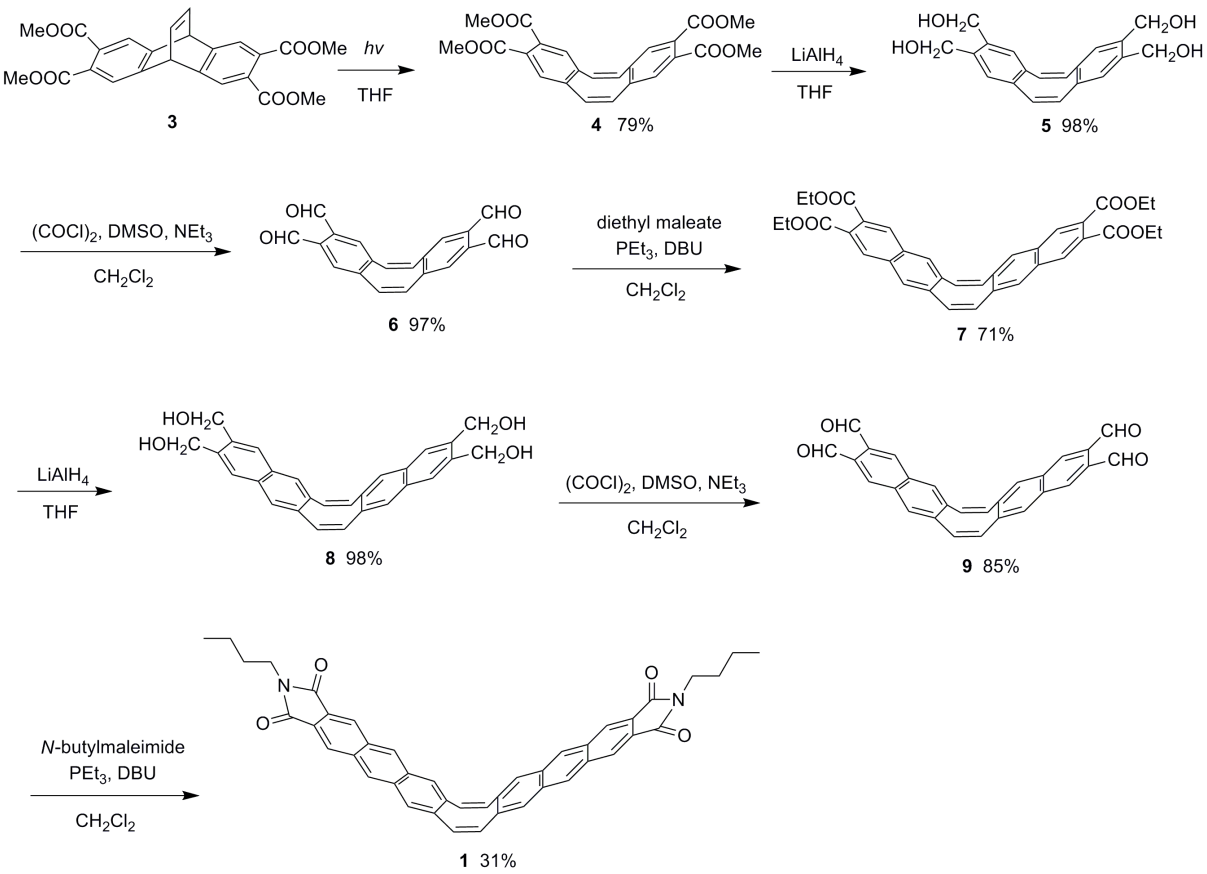

Scheme S1. Synthesis of anthraceneimide dimer **1**.

General procedure A: Reduction of tetraesters to tetraols (4 → 5 and 7 → 8)

To a solution of tetraester in THF was added a suspension of $LiAlH_4$ (8 equiv) in THF dropwise at 0 °C. After being stirred at room temperature for 12 h, the reaction was quenched with saturated Na_2SO_4 solution, which produced a white gel. A 1 M HCl aqueous solution was added to the reaction mixture after evaporation of THF. The resulting suspension was filtered, washed with water and dried under reduced pressure to afford the corresponding tetraol.

General procedure B: Swern oxidation of tetraols to tetraaldehydes (5 → 6 and 8 → 9)

To a stirred CH_2Cl_2 solution of oxalyl chloride (12 equiv, oxalyl chloride/CH_2Cl_2 = 1/10 in the ratio of volume) was added a CH_2Cl_2 solution of DMSO (14 equiv, DMSO/CH_2Cl_2 = 1/2 in the ratio of volume) dropwise at −78 °C under a nitrogen atmosphere and the stirring was continued for 30 min. Then, a solution of tetraol in DMSO/CH_2Cl_2 (1/2 in the ratio of volume)

mixture was slowly added and the reaction mixture was further stirred for 6 h at −78 °C. The reaction was quenched by the dropwise addition of triethylamine (20 equiv) and then warmed to room temperature in 1 h. Water was added and the reaction mixture was extracted with CH_2Cl_2 three times. The combined organic layer was washed with water, dried over anhydrous Na_2SO_4, and concentrated under reduced pressure to afford the corresponding tetraaldehyde. Due to their instability, the obtained tetraaldehyde compounds were used for the next reaction without further purification.

General procedure C: Homologation from tetraaldehydes to π-extended tetraester or diimide[2,4] (6 → 7 and 9 → 1)

To a CH_2Cl_2 solution of diethyl maleate (2.4 equiv) was added tri-*n*-butylphosphine (2.6 equiv) dropwise at 0 °C under nitrogen atmosphere. The reaction mixture was stirred at room temperature for 30 min. The Wittig reagent thus generated was added dropwise to a CH_2Cl_2 solution of tetraaldehyde at 0 °C under a nitrogen atmosphere. Then, DBU (0.1 equiv) was added dropwise to the reaction mixture. The reaction mixture was stirred for 12 h at room temperature. The reaction was quenched with water and extracted with CH_2Cl_2 three times. The combined organic layer was dried over anhydrous Na_2SO_4 and concentrated under reduced pressure. The mixture was purified by a silica gel column chromatography to afford π-extended tetraester. A similar procedure was employed for the synthesis of π-extended diimide using *n*-butylmaleimide in place of diethyl maleate.

Tetrakis(methoxycarbonyl)dibenzo[*a,e*]cyclooctatetraene 4. A solution of **3** (436 mg, 1.00 mmol) in degassed anhydrous THF (1.0 L) was irradiated with a high-pressure mercury lamp (450 W) at room temperature for 3 h under a nitrogen atmosphere. After evaporation of the solvent, the mixture was purified by a silica gel column chromatography using CH_2Cl_2/EtOAc (30/1 in the ratio of volume, R_f = 0.45) as an eluent to afford **4** (344 mg, 0.79 mmol) in 79% yield as a white solid. mp: 179.2−181.0 °C; ^{1}H NMR (400 MHz, $CDCl_3$): δ 7.42 (s, 4H), 6.81 (s, 4H), 3.86 (s, 12H); ^{13}C NMR (100 MHz, $CDCl_3$): δ 167.6, 139.7, 133.4, 130.7, 129.9, 52.8; HRMS (APCI, positive): [(M+H)$^+$] calcd for $C_{24}H_{21}O_8$, 437.1231; found 437.1240.

Tetrakis(hydroxymethyl)dibenzo[*a,e*]cyclooctatetraene 5: Synthesis of **5** was carried out according to General procedure A using the following quantities of reagents: compound **4** (1.75 g, 4.00 mmol) in 40 mL THF and $LiAlH_4$ (1.21 g, 32.0 mmol) in 32 mL THF. The product **5** was obtained (1.27 g, 3.92 mmol) in 98% yield as a white solid. mp: 245.0 °C (decomposed); ^{1}H NMR (400 MHz, DMSO-d_6): δ 7.04 (s, 4H), 6.73 (s, 4H), 5.01 (t, J = 5.6 Hz, 4H, –$CH_2O\underline{H}$), 4.43 (d, J = 5.6 Hz, 8H, –$C\underline{H_2}OH$); ^{13}C NMR (100 MHz, DMSO-d_6): δ 138.1, 135.1, 133.1, 127.3, 60.0; HRMS (APCI, positive): [(M+DMSO+H)$^+$] calcd for $C_{22}H_{27}O_5S$, 403.1574; found 403.1564.

Tetraformyldibenzo[*a,e*]cyclooctatetraene 6: Synthesis of **6** was carried out according to General procedure B using the following quantities of reagents: compound **5** (1.95 g, 6.00 mmol) in 120 mL DMSO/CH_2Cl_2 (1/2 in the ratio of volume), oxalyl chloride (6.0 mL, 72.0 mmol) in 60 mL CH_2Cl_2, DMSO (14.3 mL, 84.0 mmol) in 30 mL CH_2Cl_2, and triethylamine (16.5 mL, 120 mmol). The product **6** (1.84 g, 5.82 mmol) was obtained in 97% yield as a light yellow solid. mp: 221.0 °C (decomposed); ^{1}H NMR (400 MHz, $CDCl_3$) δ 10.44 (s, 4H, –$C\underline{H}O$), 7.68 (s, 4H), 6.96 (s, 4H); ^{13}C NMR (100 MHz, $CDCl_3$): δ 191.7, 142.1, 135.1, 133.8, 132.6; HRMS (APCI, positive): [(M+H)$^+$] calcd for $C_{20}H_{13}O_4$, 317.0808; found 317.0802.

Tetrakis(ethoxycarbonyl)-substituted naphthalene dimer 7: Synthesis of **7** was carried out according to General procedure C using the following quantities of reagents: compound **6** (0.95 g, 3.00 mmol), diethyl maleate (1.16 mL, 7.20 mmol), tri-*n*-butylphosphine (1.95 mL, 7.80 mmol), DBU (0.045 mL, 0.30 mmol), and CH_2Cl_2 (150 mL). The resulting mixture was purified by a silica gel column chromatography using CH_2Cl_2 (R_f = 0.50) as an eluent to afford **7** (1.26 g, 2.13 mmol) in 71% yield as a white solid. mp: 212.1–213.4 °C; ^{1}H NMR (400 MHz, $CDCl_3$) δ 8.09 (s, 4H), 7.66 (s, 4H), 7.08 (s, 4H), 4.37 (q, J = 7.2 Hz, 8H), 1.37 (t, J = 7.2 Hz, 12H); ^{13}C NMR (100 MHz, $CDCl_3$): δ 167.7, 137.4, 133.4, 132.2, 129.8, 129.1, 128.8, 61.7, 14.3; HRMS (APCI, positive): [(M+H)$^+$] calcd for $C_{36}H_{33}O_8$, 593.2170; found 593.2185.

Tetrakis(hydroxymethyl)-substituted naphthalene dimer 8: Synthesis of **8** was carried out according to General procedure A using the following quantities of reagents: compound **7** (1.12 g, 1.90 mmol) in 190 mL THF and $LiAlH_4$ (0.58 g, 15.2 mmol) in 15 mL THF. The product **8** was obtained (0.79 g, 1.86 mmol) in 98% yield as a white solid. mp: 243.9 °C (decomposed); ^{1}H NMR (400 MHz, DMSO-d_6): δ 7.76 (s, 4H), 7.65 (s, 4H), 7.04 (s, 4H), 5.20 (t, J = 5.6 Hz, 4H, –$CH_2O\underline{H}$), 4.62 (d, J = 5.6 Hz, 8H, –$C\underline{H_2}OH$); ^{13}C NMR (100 MHz, DMSO-d_6): δ 138.5, 134.1, 132.9, 130.9, 127.4, 124.3, 60.5; HRMS (APCI, positive): [(M+DMSO+H)$^+$] calcd for $C_{30}H_{31}O_5S$, 503.1887; found 503.1902.

Tetraformyl-substituted naphthalene dimer 9: Synthesis of **9** was carried out according to General procedure B using the following quantities of reagents: compound **8** (0.76 g, 1.80 mmol) in 180 mL DMSO/CH_2Cl_2 (1/2 in the ratio of volume), oxalyl chloride (1.80 mL, 21.6 mmol) in 20 mL CH_2Cl_2, DMSO (4.30 mL, 25.2 mmol) in 10 mL CH_2Cl_2, and triethylamine (5.0 mL, 36.0 mmol). The product **9** (0.64 g, 1.53 mmol) was obtained in 85% yield as a light yellow solid. mp: 222.4 °C (decomposed); ^{1}H NMR (400 MHz, $CDCl_3$): δ 10.56 (s, 4H, –$C\underline{H}O$), 8.31 (s, 4H), 7.83 (s, 4H), 7.17 (s, 4H); ^{13}C NMR (100 MHz, $CDCl_3$): δ 192.3, 138.9, 134.2, 133.6, 133.3, 133.2, 129.9; HRMS (APCI, positive): [(M+H)$^+$] calcd for $C_{28}H_{17}O_4$, 417.1121; found 417.1129.

Anthraceneimide dimer 1: Synthesis of **1** was carried out according to General procedure C using the following quantities of reagents: compound **9** (416 mg, 1.00 mmol), *N*-butylmaleimide (368 mg, 2.40 mmol), tri-*n*-butylphosphine (0.65 mL, 2.60 mmol), DBU (0.015 mL, 0.10 mmol), and CH_2Cl_2 (400 mL). The resulting mixture was purified by a silica gel column chromatography using CH_2Cl_2/AcOEt (100/1 in the ratio of volume, R_f = 0.25) as an eluent to afford **1** (203 mg, 0.31 mmol) in 31% yield as a yellow solid. mp: 224.5 °C (decomposed); ^{1}H NMR (400 MHz, *o*-dichlorobenzene-d_4, 160 °C): δ 8.21 (s, 4H), 8.18 (s, 4H), 7.72 (s, 4H), 7.11 (s, 4H), 3.71 (t, J = 7.2 Hz, 4H), 1.68–1.72 (m, 4H), 1.32–1.36 (m, 4H), 0.88 (t, J = 7.2 Hz, 6H); The ^{13}C NMR spectrum was not obtained due to its poor solubility in common organic solvents; HRMS (APCI, positive): [(M+H)$^+$] calcd for

$C_{44}H_{35}N_2O_4$, 655.2591; found 655.2586.

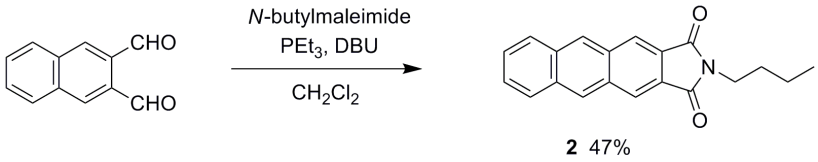

Scheme S2. Synthesis of *N*-butylanthraceneimide **2**.

***N*-Butylanthraceneimide** (**2**): Synthesis of **2** was carried out according to General procedure C using the following quantities of reagents: naphthalene-2,3-dicarbaldehyde (184 mg, 1.0 mmol), *N*-butylmaleimide (184 mg, 1.20 mmol), tri-*n*-butylphosphine (0.33 mL, 1.3 mmol), DBU (0.015 mL, 0.10 mmol), and CH_2Cl_2 (10 mL). The mixture was purified by a silica gel column chromatography using hexane/CH_2Cl_2 (1/2 in the ratio of volume, R_f = 0.24) as an eluent to afford **2** (203 mg, 0.31 mmol) in 47% yield as a yellow solid. mp: 203.8–204.4 °C; ^{1}H NMR (400 MHz, $CDCl_3$): δ 8.60 (s, 2H), 8.47 (s, 2H), 8.07 (dd, 2H, J_1 = 6.4 and J_2 = 3.6 Hz), 7.61 (dd, 2H, J_1 = 6.8 and J_2 = 3.2 Hz), 3.78 (t, J = 7.2 Hz, 2H), 1.71–1.75 (m, 2H), 1.39–1.45 (m, 2H), 0.98 (t, J = 7.2 Hz, 3H); ^{13}C NMR (100 MHz, $CDCl_3$): δ 168.0, 133.3, 132.1, 130.1, 128.6, 127.6, 126.9, 125.7, 38.3, 30.7, 20.3, 13.8; HRMS (APCI, positive): [(M+H)$^+$] calcd for $C_{20}H_{18}NO_2$, 304.1332; found 304.1341.

2. X-ray crystallographic analysis

Crystallographic data have been deposited with the Cambridge Crystallographic Data Center as CCDC-921157 (**1**) and CCDC-921158 (**2**). These data can be obtained free of charge from www.ccdc.cam.ac.uk/data_request/cif.

Compound 1. Orange and prism single crystals of **1** were obtained by recrystallization from a hot solution in *o*-dichlorobenzene. The measurement was performed using synchrotron radiation (λ = 0.8000 Å) at the BL38B1 in the SPring-8 with approval of the Japan Synchrotron Radiation Research Institute (JASRI) (proposal No. 2012B1324). The oscillation angle and camera distance were 1° and 75 mm, respectively. The exposure time per frame was 15 s. Data sets of 180 frames were integrated, scaled, and merged with the HKL2000 program.[S2] The structure was solved by direct methods (SHELXS-97) and refined by least-squares calculations on F^2 for all reflections (SHELXL-97) using the crystallographic software package CrystalStructure (Rigaku, CrystalStructure version 4.0. Rigaku Corporation, Tokyo, Japan, 2010). All non-hydrogen atoms were refined anisotropically and all hydrogen atoms were placed using AFIX instructions.

Total 17851 reflections were collected, among which 5037 reflections were independent (R_{int} = 0.039). Space group $P2_1/c$, a = 4.67790(10), b = 12.8530(2), c = 53.3818(7) Å, β = 91.8752 °, V = 3207.86(10) Å^3, Z = 4, T = 123 K, R_1 = 0.0531 ($I > 2\sigma(I)$), wR_2 = 0.1356 (all data), GOF = 1.116.

Compound 2. Yellow and prism single crystals of **2** were obtained by slow evaporation of a hexane/CH_2Cl_2 solution. The measurement was performed at 123 K with a Rigaku X-ray diffractometer equipped with a molybdenum MicroMax-007 microfocus generator ($\lambda_{MoK\alpha}$ = 0.7107 Å), VariMax-Mo optics, and a Saturn 70 CCD detector. The oscillation angle and camera distance were 0.5° and 45 mm, respectively. The exposure time per frame was 16 s. Data sets of 720 frames were integrated and scaled with the CrystalClear program (Rigaku, CrystalClear version 1.3.6. Rigaku Corporation, Tokyo, Japan, 2006). The structure was solved by direct methods (SHELXS-97) and refined by least-squares calculations on F^2 for all reflections (SHELXL-97) using the crystallographic software packages CrystalStructure. All non-hydrogen atoms were refined anisotropically and all hydrogen atoms were placed using AFIX instructions.

Total 9076 reflections were collected, among which 2489 reflections were independent (R_{int} = 0.0199). Space group $P2_1/c$, a = 17.309(2), b = 11.5835(14), c = 7.4963(9) Å, β = 101.442(2) °, V = 1473.1(3) Å^3, Z = 4, T = 123 K, R_1 = 0.0388 ($I > 2\sigma(I)$), wR_2 = 0.1035 (all data), GOF = 1.047.

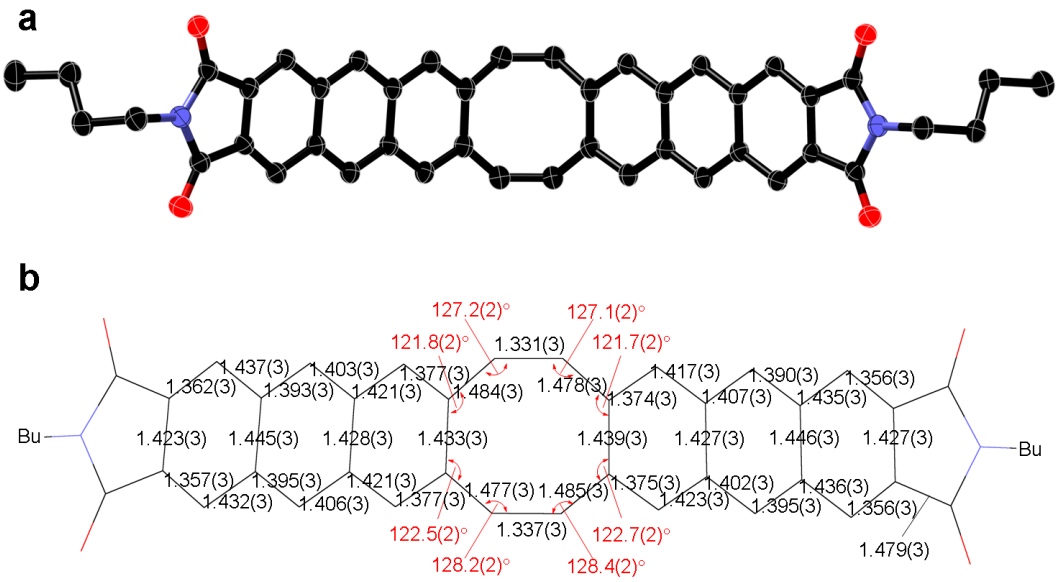

Figure S1. Molecular geometry and structural parameters of **1** in the crystal. (a) Thermal ellipsoid plot with 50% probability. (b) Bond lengths (Å) and bond angles (°).

3. Photophysical properties

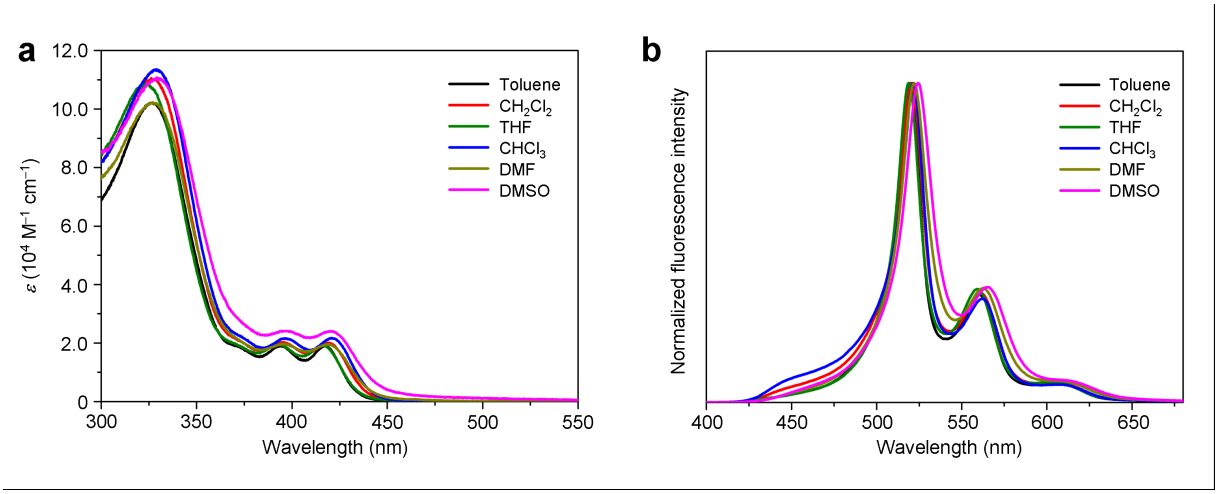

Figure S2. Photophysical properties of **1** in various solvents. (a) UV-vis absorption spectra. (b) fluorescence spectra with the concentration of [**1**] = 5×10^{-6} M. Excitation wavelength λ_{ex} = 350 nm.

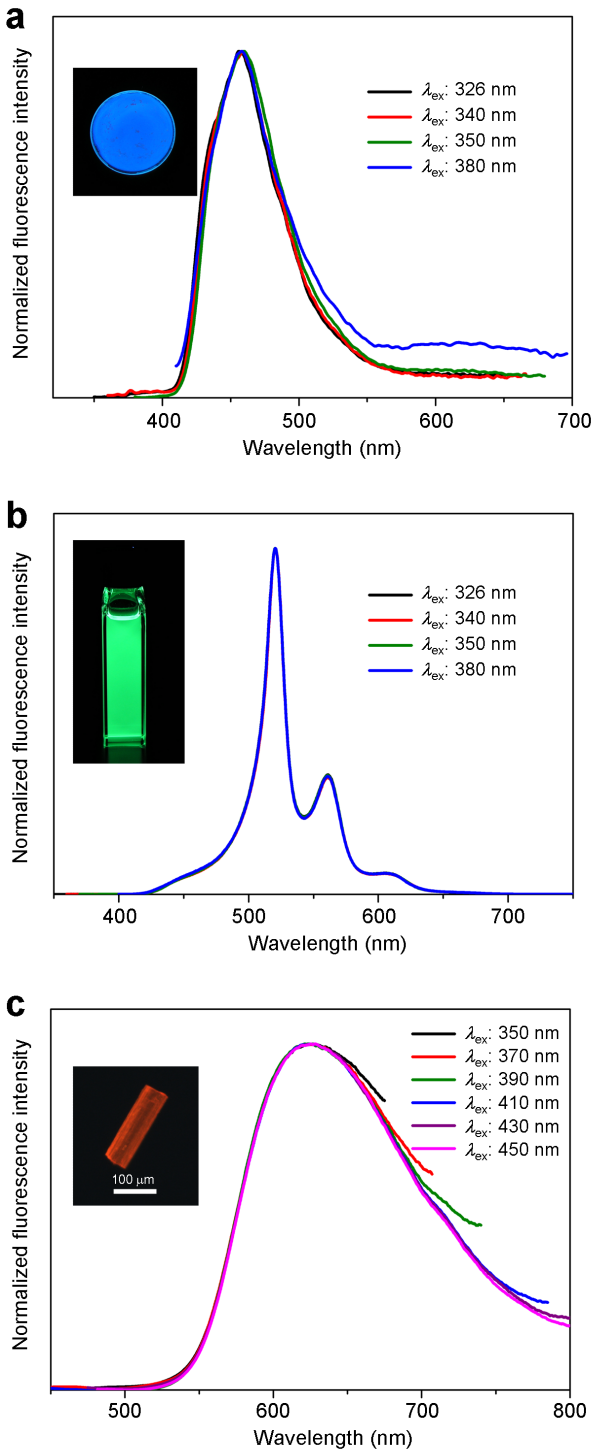

Figure S3. Fluorescence spectra of **1** under different excitation wavelengths. (a) The blue emission spectra in PMMA matrix (1 wt% ratio). (b) The green emission spectra in CH_2Cl_2 solution ([**1**] = 5×10^{-6} M). (c) The red emission spectra in the crystalline state, in which the secondary light scattering was not displayed.

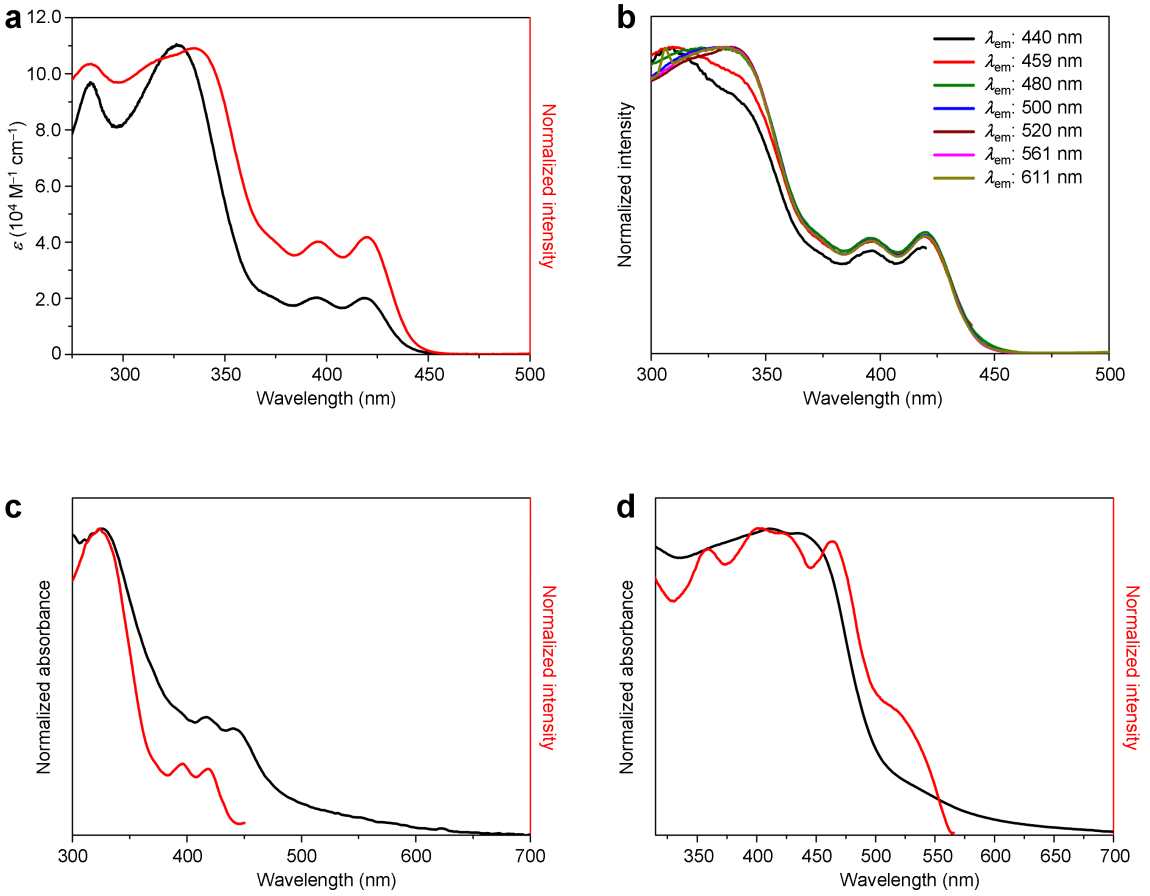

Figure S4. Absorption, excitation, and diffuse reflectance spectra of **1**. (a) UV-vis absorption (black line) and excitation (red line, monitored at λ_{em} = 520 nm) spectra of **1** in CH_2Cl_2 solution ([**1**] = 5 × 10^{-6} M). (b) Excitation spectra of **1** in a CH_2Cl_2 solution ([**1**] = 5 × 10^{-6} M) under different emission wavelengths. (c) UV-vis absorption (black line) and excitation (red line, monitored at λ_{em} = 459 nm) spectra of **1** in a PMMA matrix (1 wt% ratio). (d) Diffuse reflectance (black line) and excitation (red line, monitored at λ_{em} = 625 nm) spectra of **1** in the crystalline state.

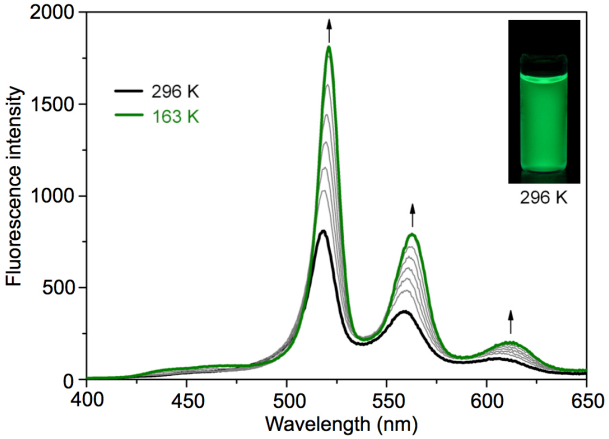

Figure S5. Temperature-dependent fluorescence of **1** in MHTF from 296 to 163 K. Excitation wavelength λ_{ex} = 350 nm.

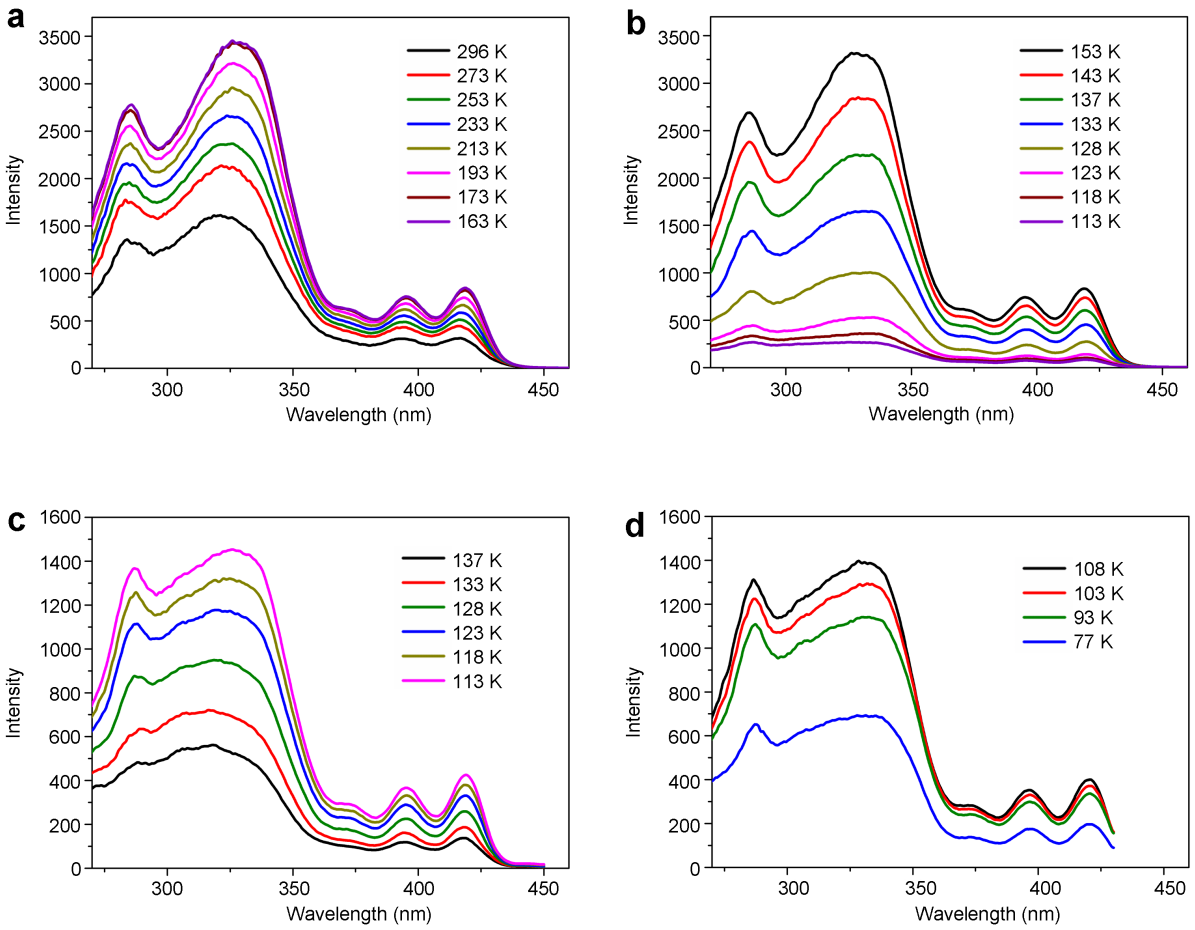

Figure S6. Excitation spectra of **1** in MHTF ([**1**] = 1×10^{-6} M) at various temperatures (a) from 296 to 163 K monitored at λ_{em} = 520 nm, (b) from 153 to 113 K monitored at λ_{em} = 520 nm, (c) from 137 to 113 K monitored at λ_{em} = 460 nm, and (d) from 108 to 77 K monitored at λ_{em} = 440 nm.

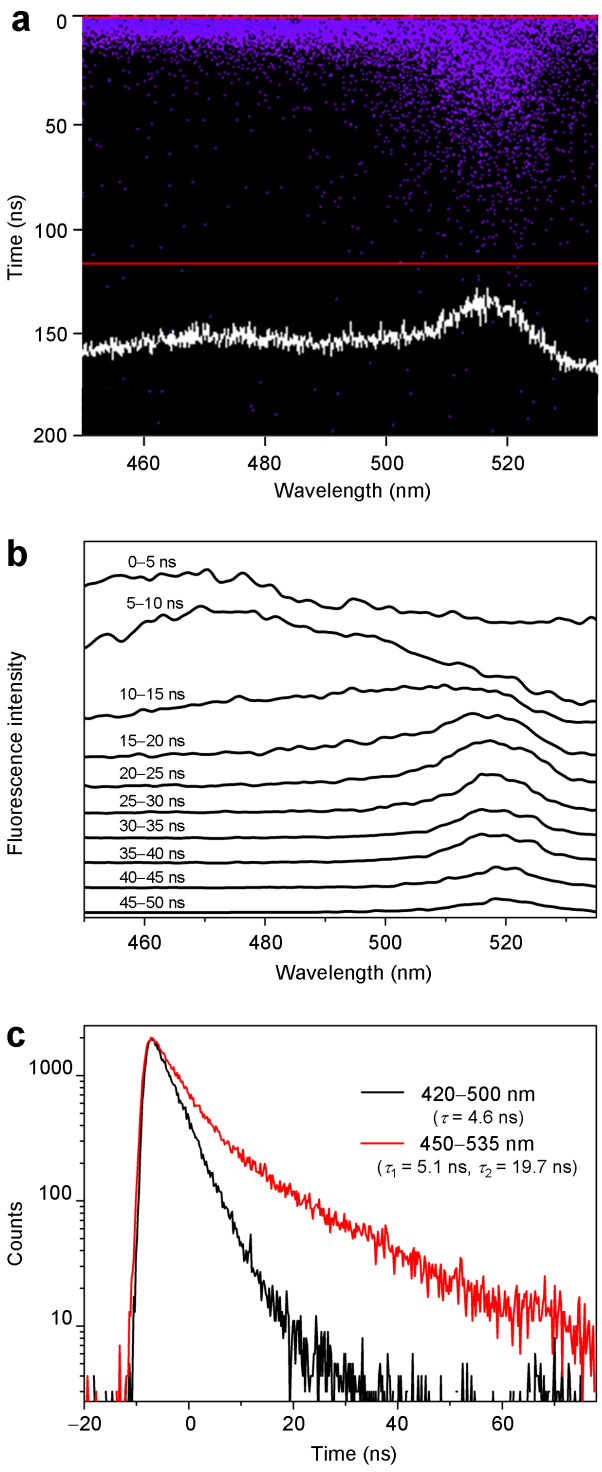

Figure S7. Time-resolved emission spectroscopy of **1** ([**1**] = 5 × 10^{-6} M in MTHF) excited at 337 nm at 133 K. (a) Streak image, where the horizontal axis corresponds to the emission wavelength and the vertical axis corresponds to the time after the excitation pulse. (b) Emission spectra that result from the integration of the streak image along the time axis within the consecutive 5 ns intervals. The spectra are offset from each other for clarity. (c) Fluorescence decays and lifetimes of the emission bands in the spectral ranges from 420–500 nm and 450–535 nm.

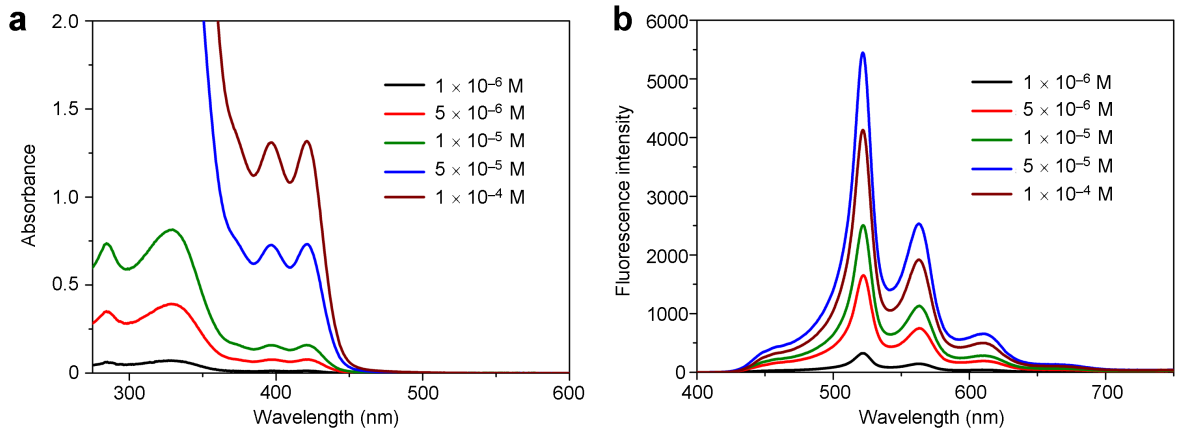

Figure S8. Concentration dependence of the photophysical properties of **1**. (a) UV-vis absorption and (b) fluorescence spectra of **1** in $CHCl_3$ solutions with different concentration. Excitation wavelength λ_{ex} = 350 nm.

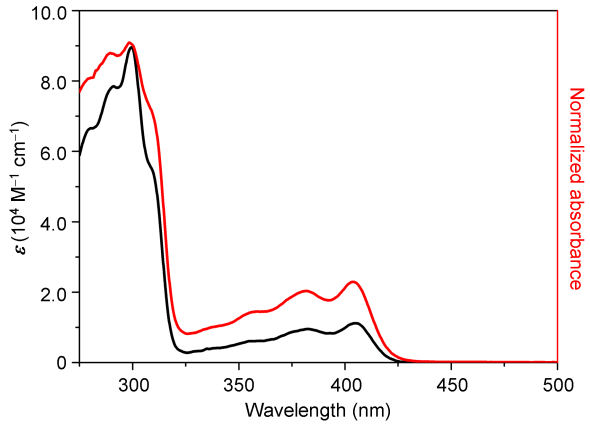

Figure S9. UV-vis absorption spectra of **2** in a CH_2Cl_2 solution (black line, [**2**] = 5 × 10^{-6} M) and in a PMMA matrix (red line, 1 wt % ratio).

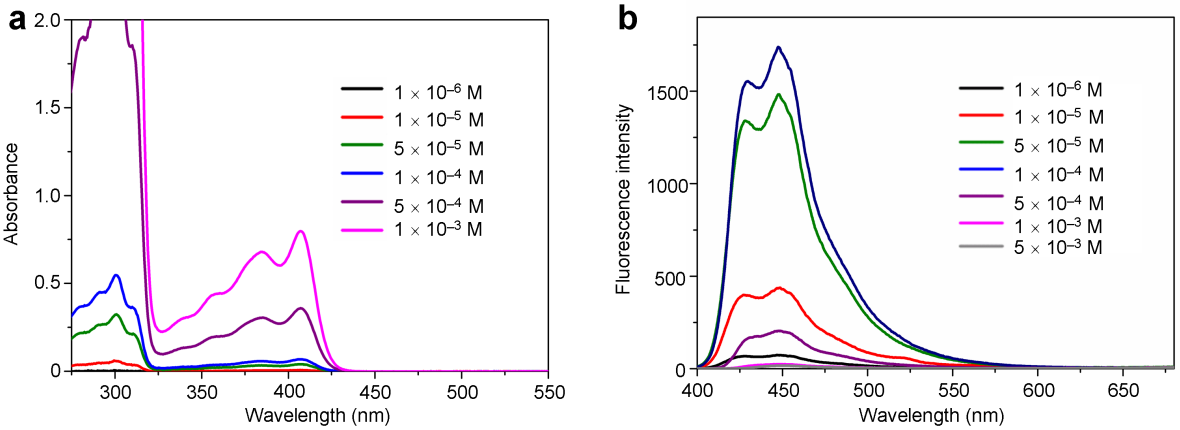

Figure S10. Concentration dependence of the photophysical properties of **2**. (a) UV-vis absorption and (b) fluorescence spectra of **2** in $CHCl_3$ solutions with different concentration. Excitation wavelength λ_{ex} = 380 nm.

Table S1. Spectral Parameters of Compounds **1** and **2** in the Absorption and Fluorescence

Cmpd	In CH_2Cl_2 solution				In PMMA matrix				In the crystalline state		
	λ_{abs} / nm[a]	λ_{em} / nm[b]	Φ_f[c]	τ / ns[d]	λ_{abs} / nm[a]	λ_{em} / nm[b]	Φ_f[c]	τ / ns[d]	λ_{em} / nm[b]	Φ_f[c]	τ / ns[d]
1	284, 326, 395, 419	459, 520, 561, 610	0.31	11.8	285, 328, 416, 442	459	0.09	8.4	625	0.06	12–14
2	299, 381, 404	425, 447	0.46	8.6	299, 381, 404	418, 440	0.41	12.1	538	0.33	88

[a]Absorption wavelength. [b]Emission wavelength. [c]Absolute fluorescence quantum yield. [d] Fluorescence lifetime.

4. Photographs of fibrous microcrystals

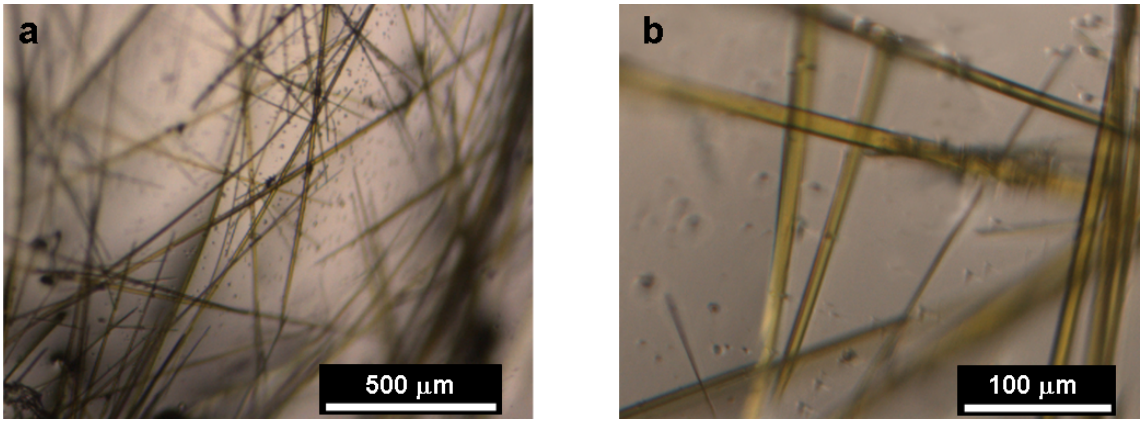

Figure S11. Photographs of fibrous microcrystals of **1** obtained by vapor diffusion of methanol into a $CHCl_3$ solution.

5. Theoretical calculations

DFT geometry optimization and TD-DFT calculations.

For all the calculations the structures **1′** and **2′** were treated, in which the *n*-butyl groups at the terminal imides of **1** and **2** are replaced with H atoms (Figure S9). The DFT geometry optimizations and the TD-DFT calculations of **1′** and **2′** were performed using the TURBOMOLE program at the PBE0/def-SV(P) level of theory. For the constrained geometry optimization of **1′** with fixed bent angle θ, the dihedral angle between the C1–C2–C3 and C2–C3–C4 planes in Figure S9 was fixed in the definition of the internal coordinates.

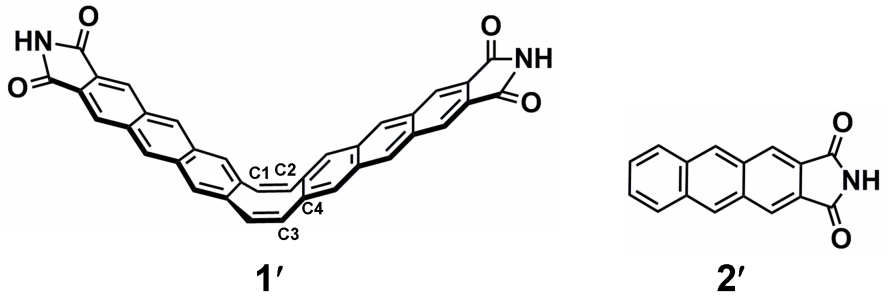

Figure S12. Chemical structures of **1′** and **2′**.

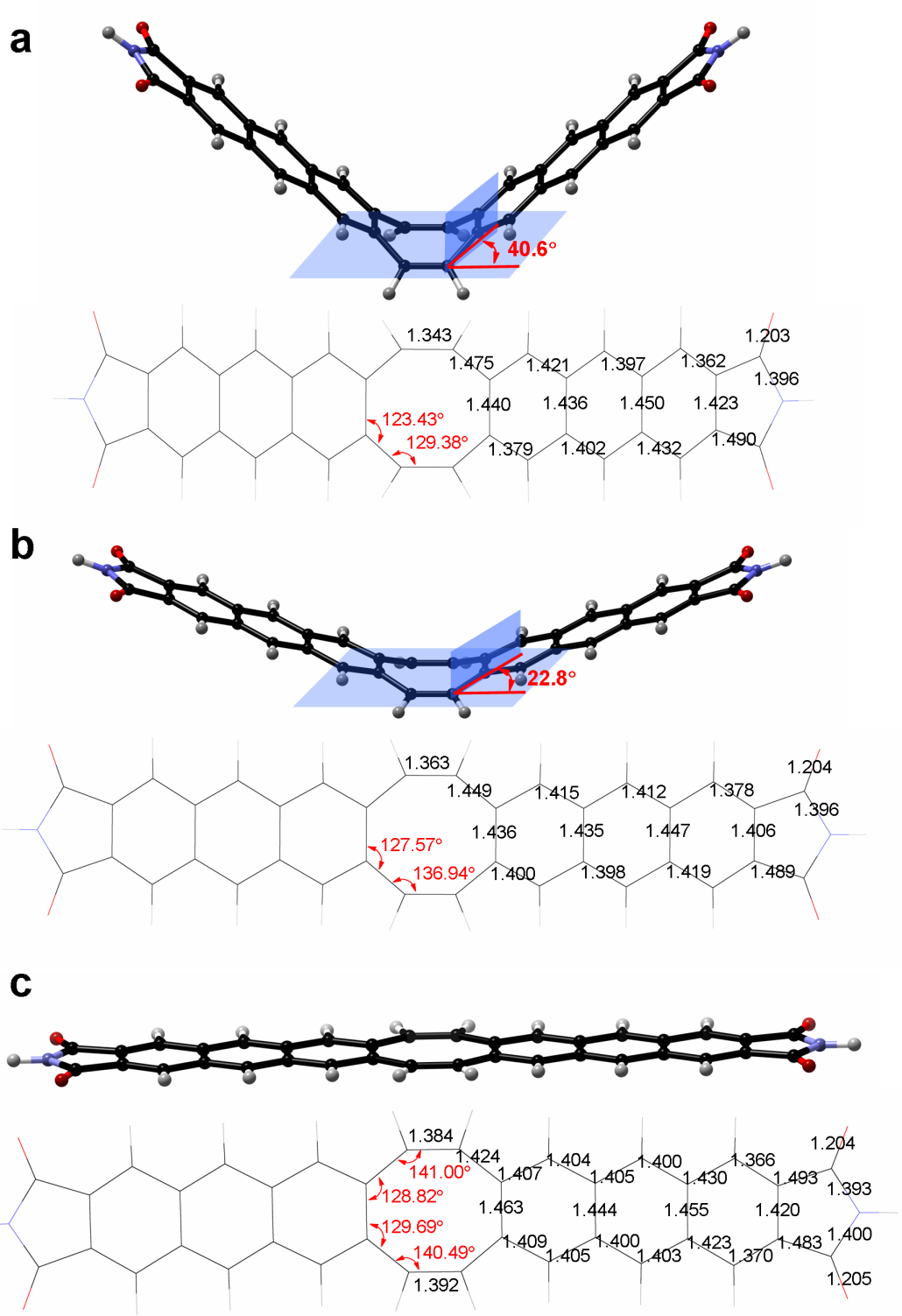

Figure S13. DFT optimized geometries of **1′**. The optimized geometry (a) in the S_0 ground state at the global minimum, (b) in the S_1 excited state at the local minimum, and (c) in the S_1 excited state at the global minimum. The geometry optimizations were performed at the PBE0/def-SV(P) level using the TURBOMOLE program.

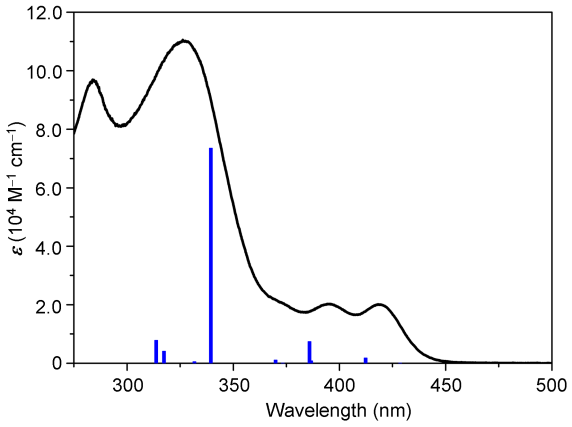

Figure S14. The oscillator strengths (blue bars) obtained by the TD-DFT calculations of **1′** at the PBE0/def-SV(P) level based on the S_0 optimized geometry and the observed UV-vis absorption spectrum (black line) of **1** in CH_2Cl_2 ([**1**] = 5.0×10^{-6} M).

Table S2. Calculated Excitations for the Optimized Geometry of **1′** in the Ground State [a]

Excited state	Transition energy / eV	Main CI coefficient	Oscillator strength *f*
1	2.893 (429 nm)	0.966 (HOMO → LUMO)	0.6208×10^{-11}
2	3.007 (412 nm)	0.924 (HOMO → LUMO+1)	0.0404
3	3.207 (387 nm)	0.926 (HOMO−1 → LUMO)	0.0180
4	3.214 (386 nm)	0.661 (HOMO → LUMO+2) 0.208 (HOMO−2 → LUMO)	0.1727
7	3.652 (339 nm)	0.730 (HOMO−2 → LUMO) 0.254 (HOMO → LUMO+2)	1.7259

[a]Calculated at the PBE0/def-SV(P) level using the TURBOMOLE program.

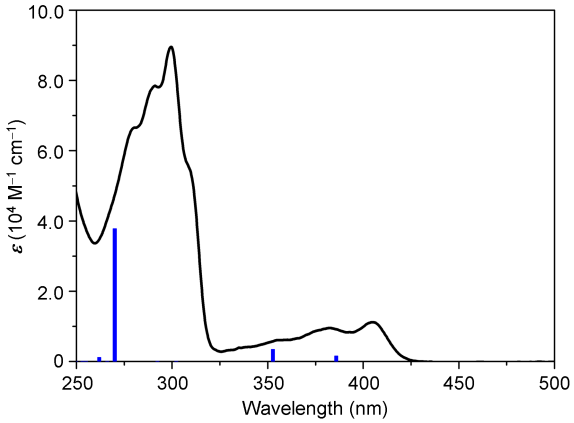

Figure S15. The oscillator strengths (blue bars) obtained by the TD-DFT calculations of **2′** at the PBE0/def-SV(P) level based on the S_0 optimized geometry and the observed UV-vis absorption spectrum (black line) of **2** in CH_2Cl_2 ([**2**] = 5.0×10^{-6} M).

Table S3. Calculated Excitations for the Optimized Geometry of **2′** in the Ground State [a]

Excited state	Transition energy / eV	Main CI coefficient	Oscillator strength *f*
1	3.213 (386 nm)	0.969 (HOMO → LUMO)	0.0437
2	3.515 (353 nm)	0.746 (HOMO → LUMO+1) 0.238 (HOMO−1 → LUMO)	0.0970
5	4.591 (270 nm)	0.594 (HOMO−1 → LUMO) 0.229 (HOMO → LUMO+1)	1.0851

[a]Calculated at the PBE0/def-SV(P) level using the TURBOMOLE program.

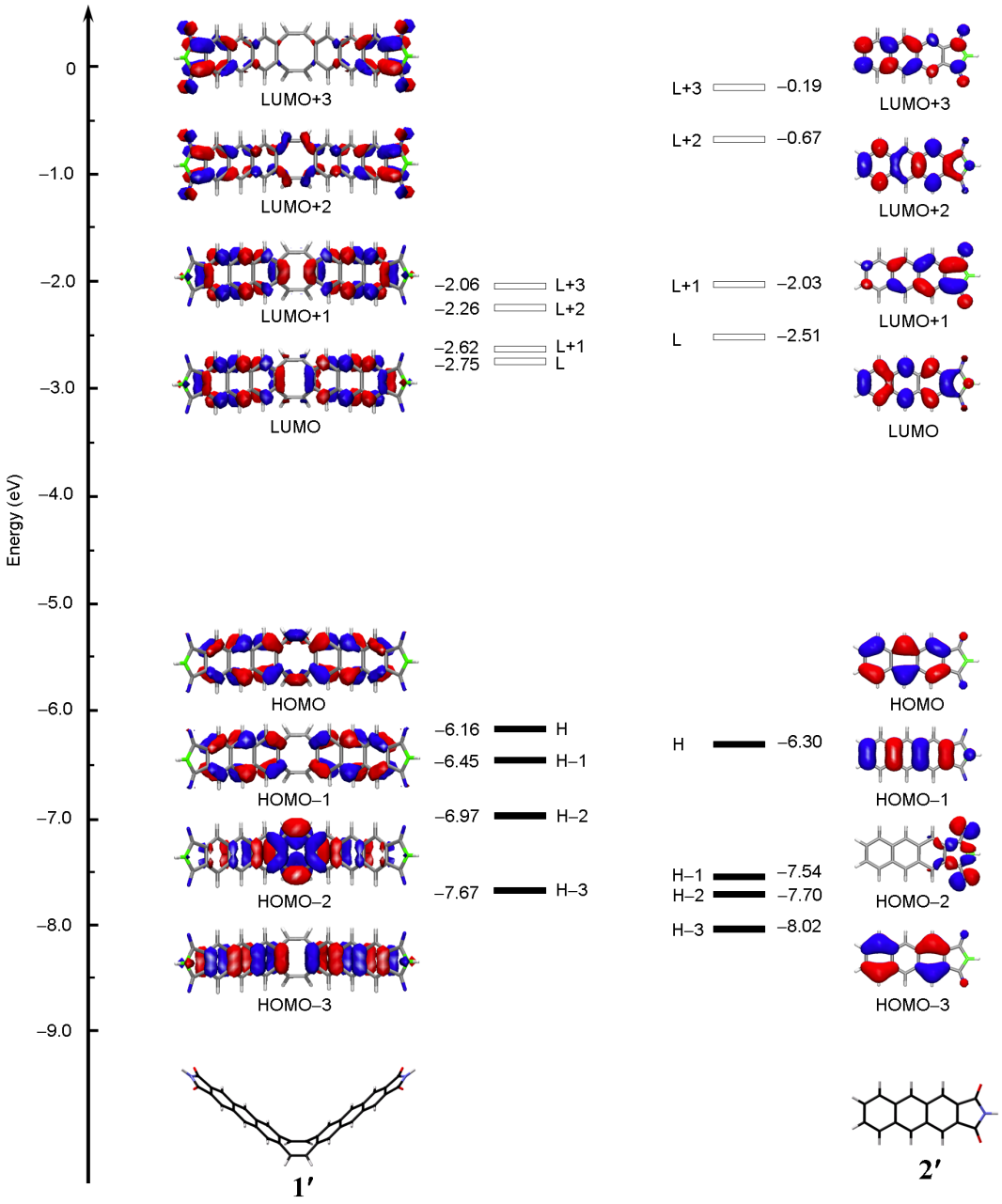

Figure S16. Kohn-Sham molecular orbitals of **1′** and **2′** based on their S_0 optimized structures calculated at the PBE0/def-SV(P) level by the TURBOMOLE program.

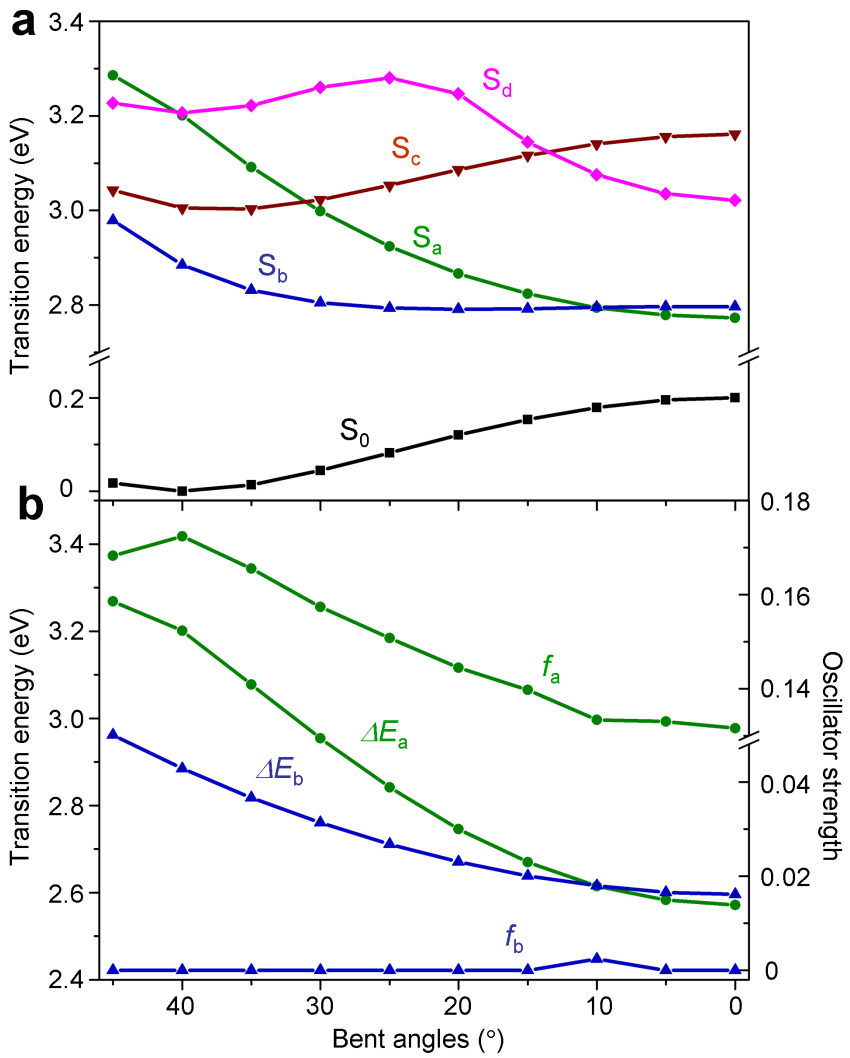

Figure S17. Calculated potential energy diagram based on the optimized geometries in the S_0 ground state. (a) Energy levels of the ground state S_0 and excited states S_a, S_b, S_c and S_d for **1′** with fixed bent angles of the COT moiety. The molecular geometries are optimized for the S_0 ground state by the TURBOMOLE program at the PBE0/def-SV(P) level. The energy levels of the excited states are obtained from the TD-DFT calculations at the same level. (b) Energy gaps ΔE_a (= S_a – S_0) and ΔE_b (= S_b – S_0), and oscillator strengths f_a for the $S_0 \rightarrow S_a$ and f_b for the $S_0 \rightarrow S_b$ transitions, respectively.

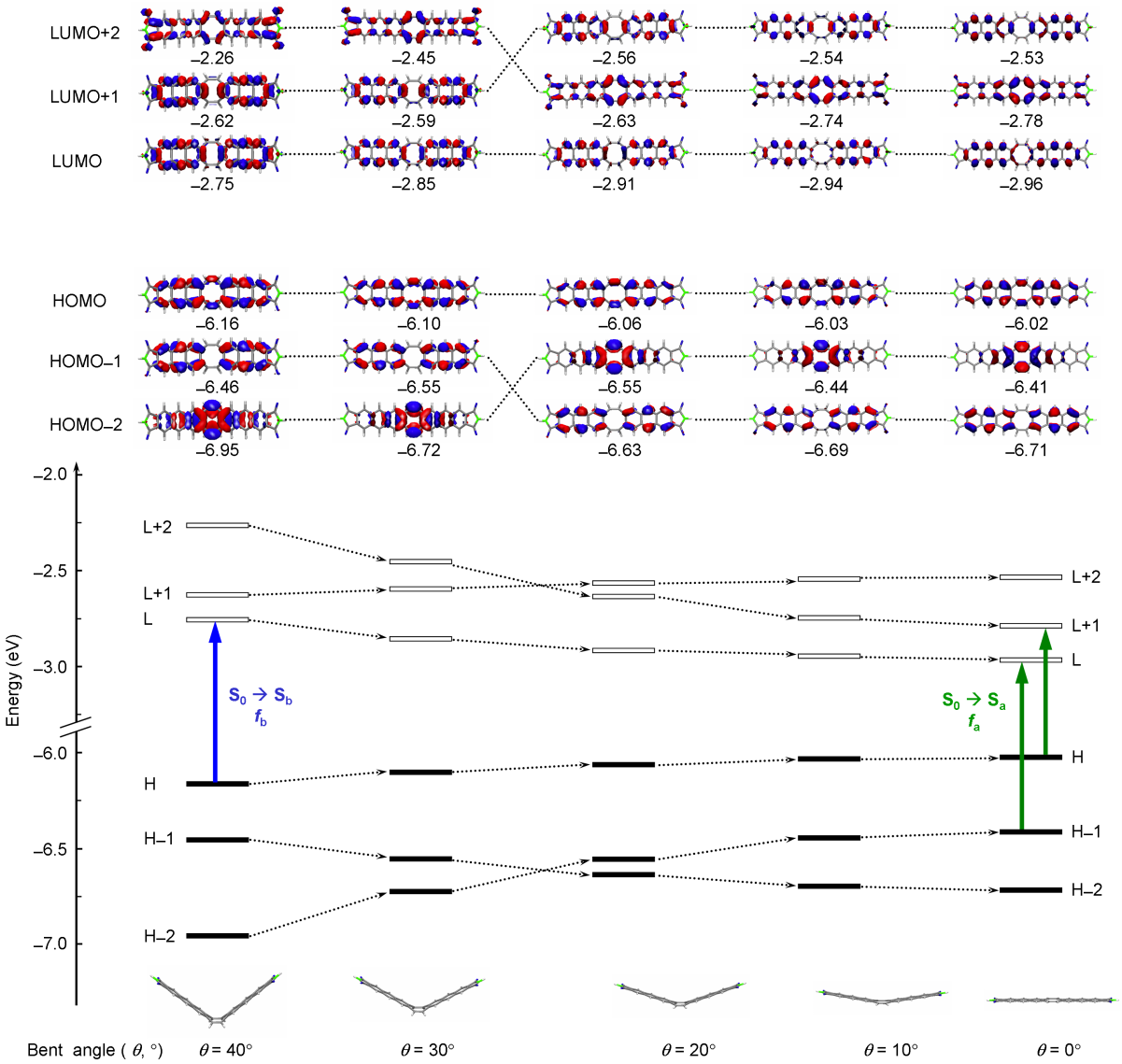

Figure S18. Kohn-Sham molecular orbitals and their energy levels of **1′** with different bent angles. The optimized geometries in the S_0 ground states were used for the calculations at the TD-PBE0/def-SV(P) level by the TURBOMOLE program.

6. References

S1. Gabioud, R. & Vogel, P. The 7,8-epoxy-2,3,5,6-tetrakis(methylene) bicyclo[2.2.2]octane: synthesis and Diels-Alder reactivity. *Tetrahedron*, **136**, 149–154 (1980).

S2. Otwinowski, Z. & Minor, W. *Methods Enzymol*. **276**, 307–326 (1997).

S3. Full notation of the Reference 13 in the manuscript: Gaussian 09, Revision C.01, Frisch, M. J.; Trucks, G. W.; Schlegel, H. B.; Scuseria, G. E.; Robb, M. A.; Cheeseman, J. R.; Scalmani, G.; Barone, V.; Mennucci, B.; Petersson, G. A.; Nakatsuji, H.; Caricato, M.; Li, X.; Hratchian, H. P.; Izmaylov, A. F.; Bloino, J.; Zheng, G.; Sonnenberg, J. L.; Hada, M.; Ehara, M.; Toyota, K.; Fukuda, R.; Hasegawa, J.; Ishida, M.; Nakajima, T.; Honda, Y.; Kitao, O.; Nakai, H.; Vreven, T.; Montgomery, Jr., J. A.; Peralta, J. E.; Ogliaro, F.; Bearpark, M.; Heyd, J. J.; Brothers, E.; Kudin, K. N.; Staroverov, V. N.; Kobayashi, R.; Normand, J.; Raghavachari, K.; Rendell, A.; Burant, J. C.; Iyengar, S. S.; Tomasi, J.; Cossi, M.; Rega, N.; Millam, J. M.; Klene, M.; Knox, J. E.; Cross, J. B.; Bakken, V.; Adamo, C.; Jaramillo, J.; Gomperts, R.; Stratmann, R. E.; Yazyev, O.; Austin, A. J.; Cammi, R.; Pomelli, C.; Ochterski, J. W.; Martin, R. L.; Morokuma, K.; Zakrzewski, V. G.; Voth, G. A.; Salvador, P.; Dannenberg, J. J.; Dapprich, S.; Daniels, A. D.; Farkas, Ö.; Foresman, J. B.; Ortiz, J. V.; Cioslowski, J.; Fox, D. J. Gaussian, Inc., Wallingford CT, 2009.

7. NMR Spectra

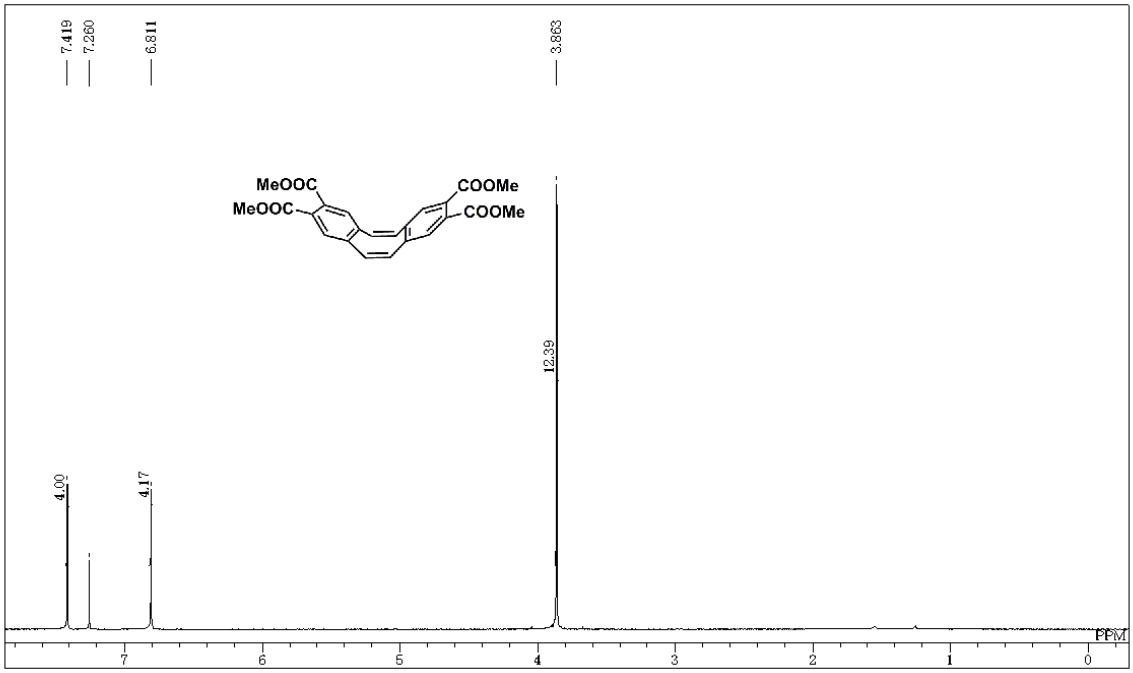

Figure S19. ^{1}H NMR spectrum of **4** in $CDCl_3$.

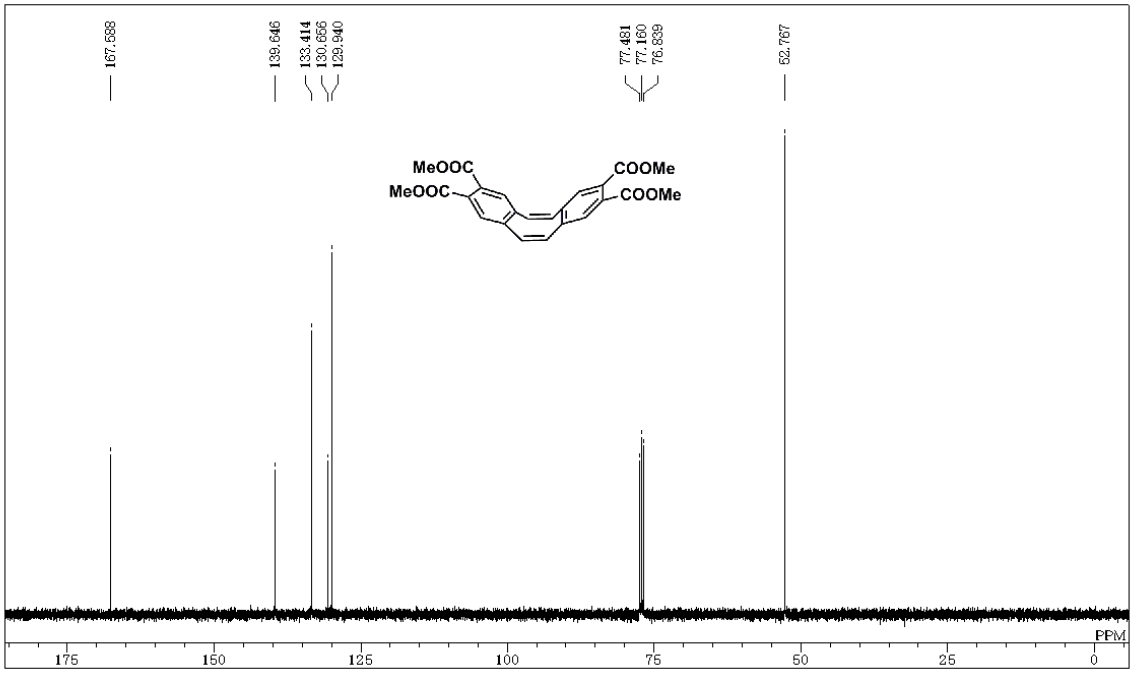

Figure S20. ^{13}C NMR spectrum of **4** in $CDCl_3$.

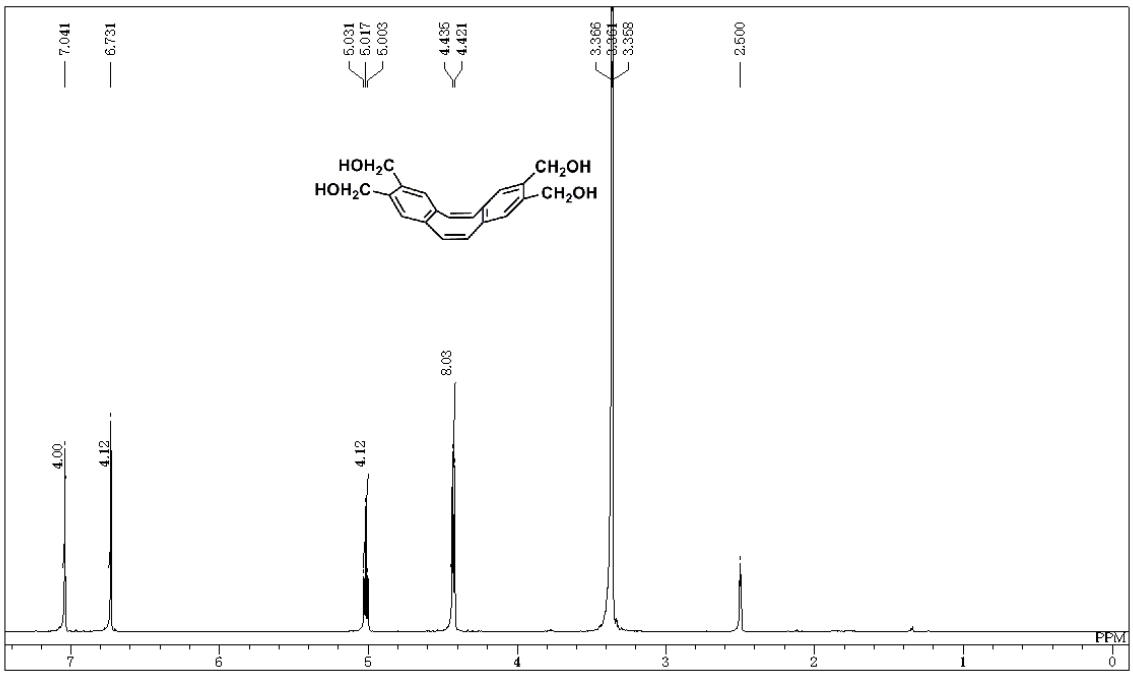

Figure S21. ^{1}H NMR spectrum of **5** in DMSO-d_6.

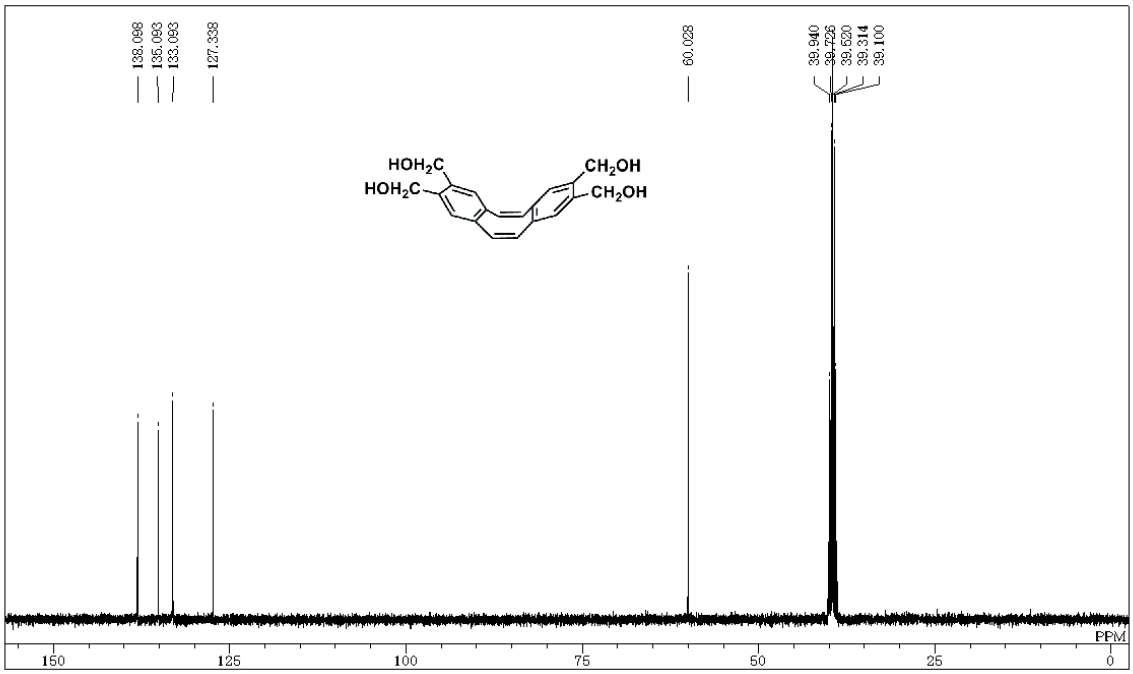

Figure S22. ^{13}C NMR spectrum of **5** in DMSO-d_6.

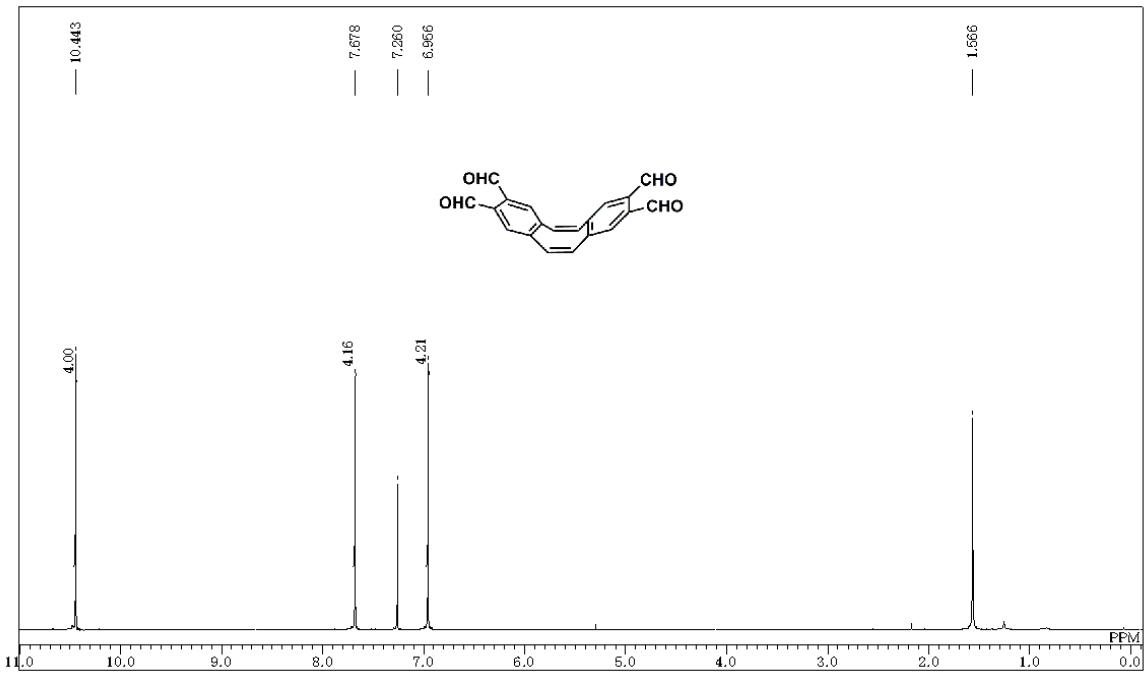

Figure S23. ^{1}H NMR spectrum of **6** in $CDCl_3$.

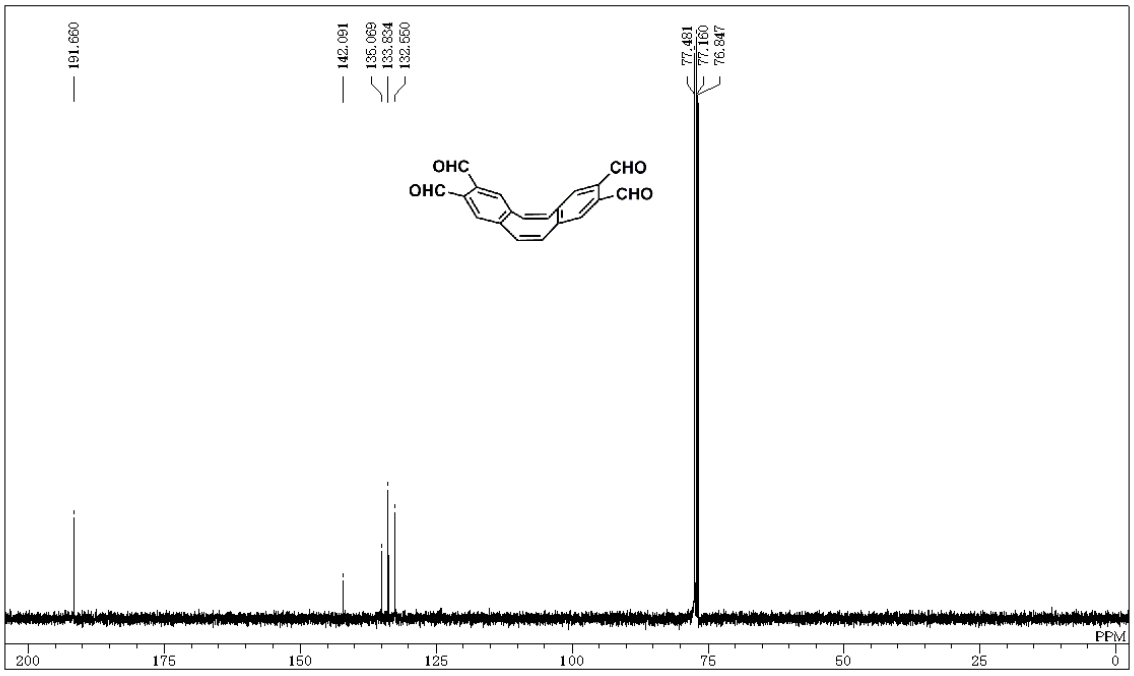

Figure S24. ^{13}C NMR spectrum of **6** in $CDCl_3$.

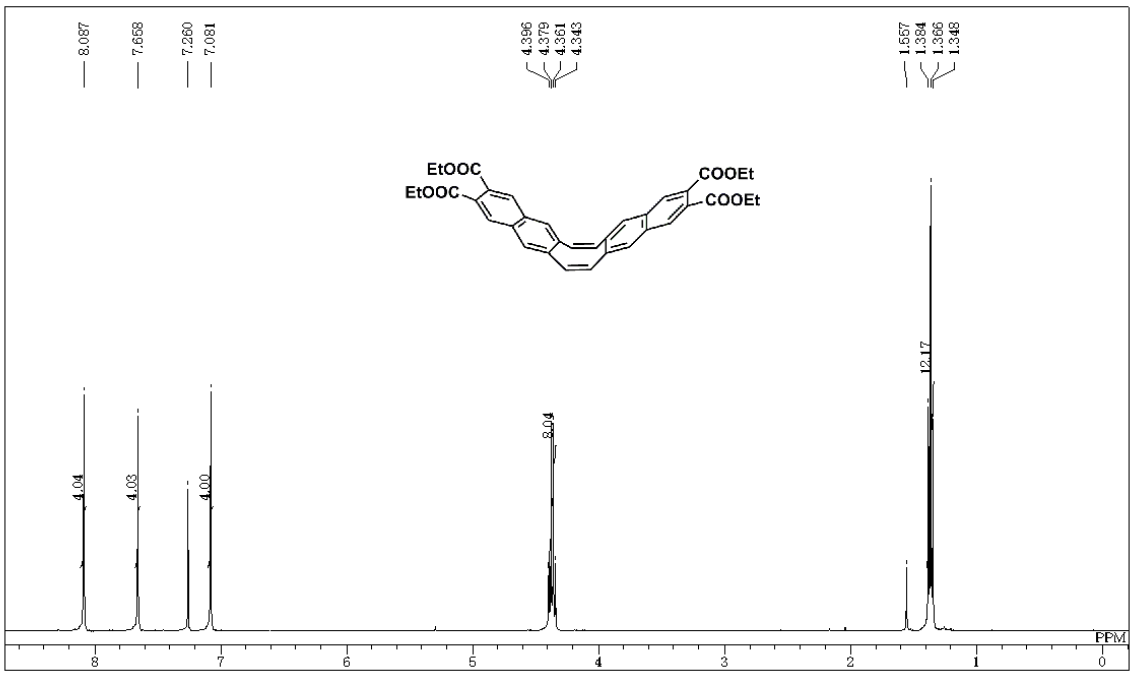

Figure S25. ^{1}H NMR spectrum of **7** in $CDCl_3$.

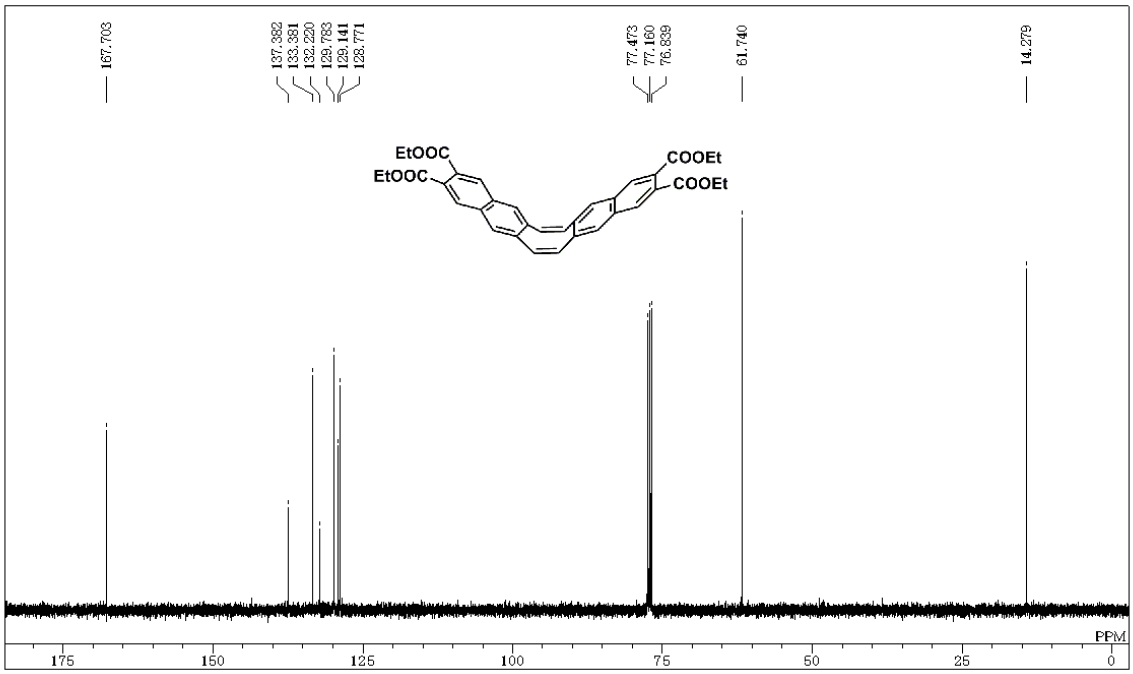

Figure S26. ^{13}C NMR spectrum of **7** in $CDCl_3$.

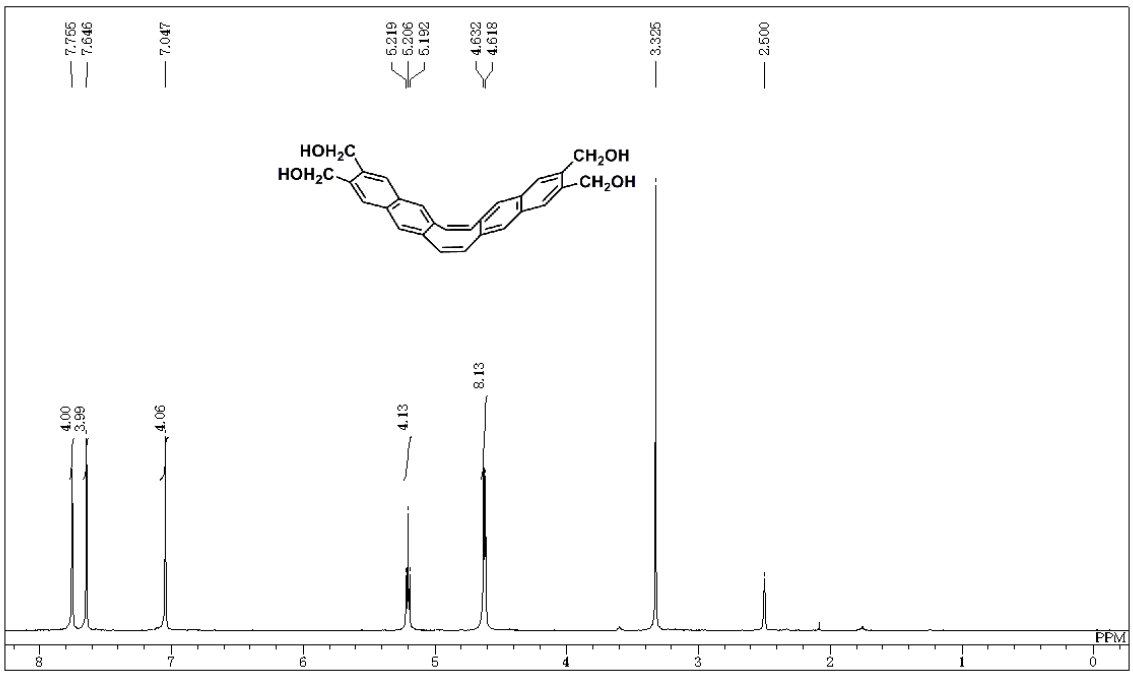

Figure S27. ^{1}H NMR spectrum of **8** in DMSO-d_6.

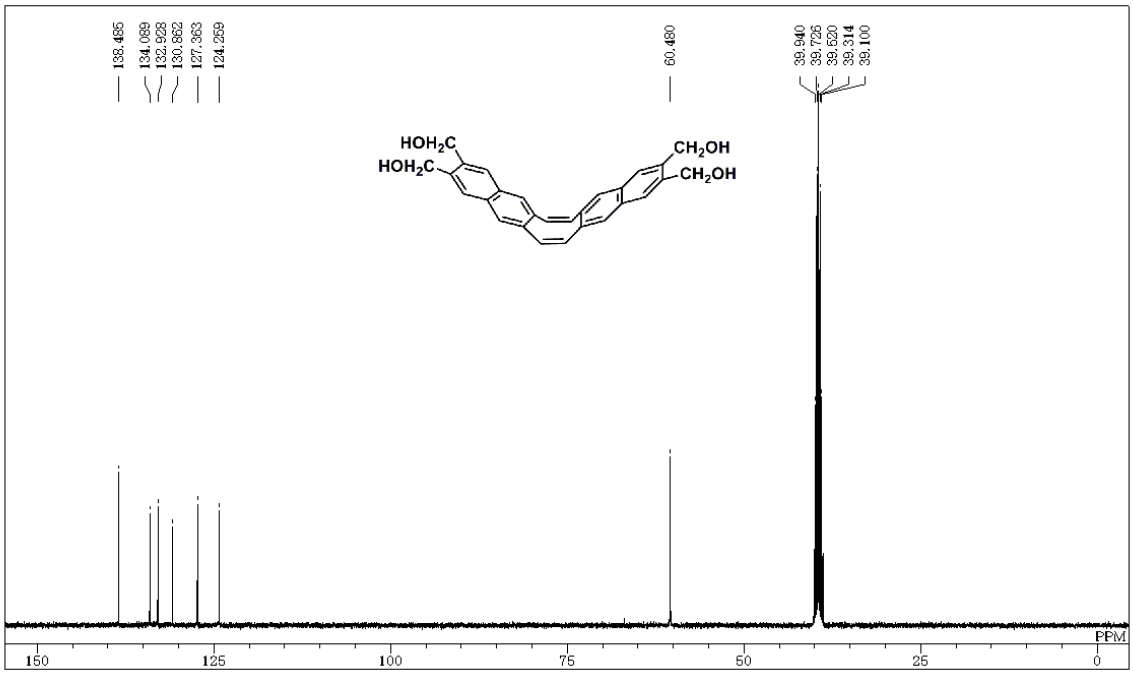

Figure S28. ^{13}C NMR spectrum of **8** in DMSO-d_6.

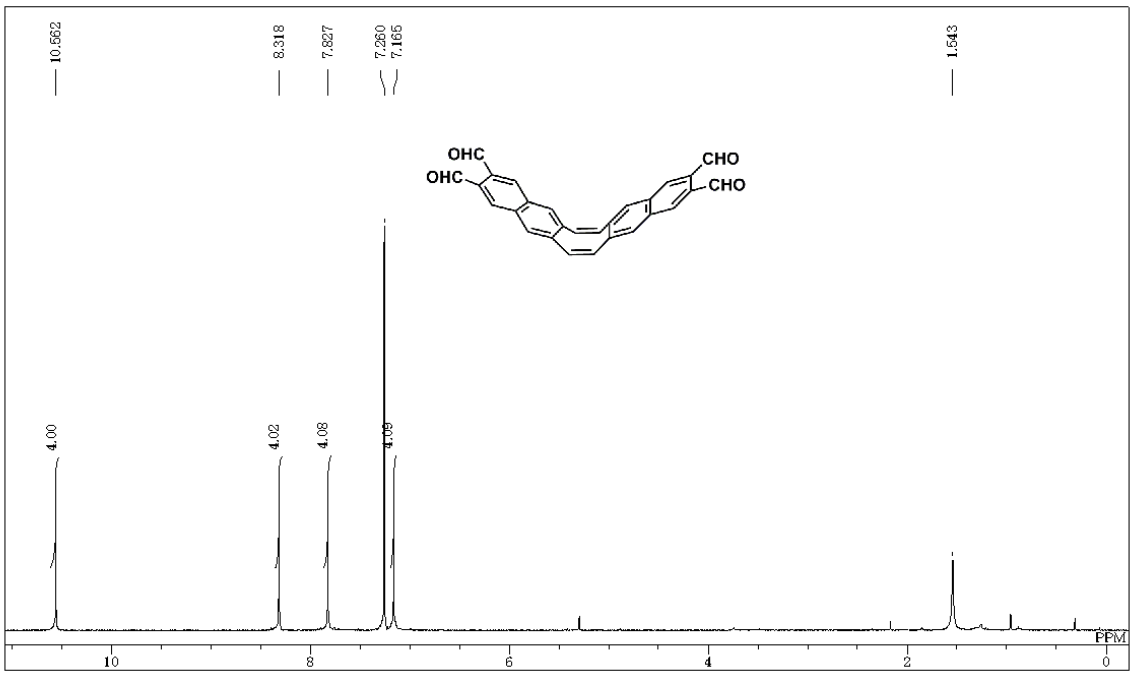

Figure S29. ^{1}H NMR spectrum of **9** in $CDCl_3$.

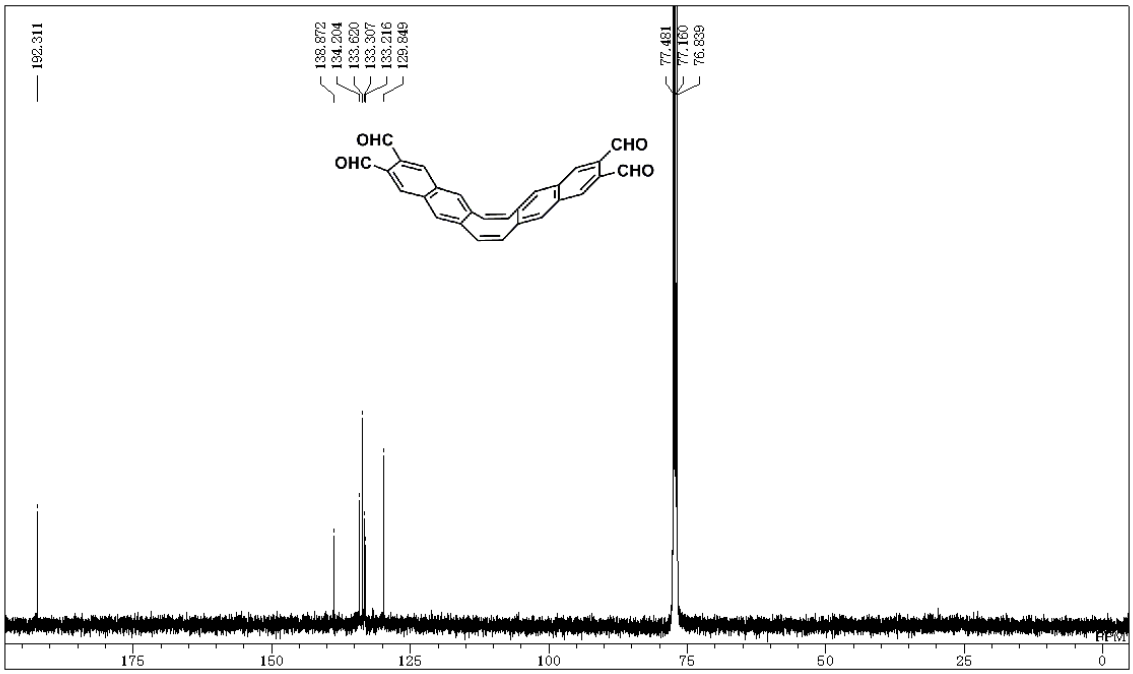

Figure S30. ^{13}C NMR spectrum of **9** in $CDCl_3$.

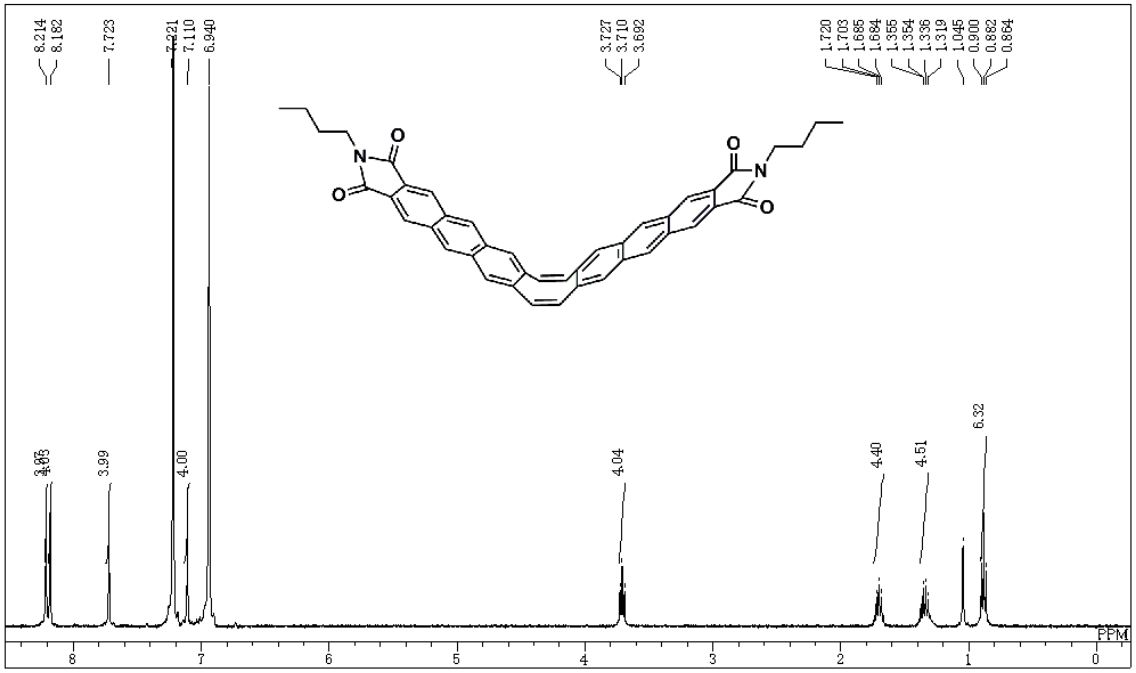

Figure S31. ^{1}H NMR spectrum of **1** in *o*-dichlorobenzene-d_4 at 160 °C.

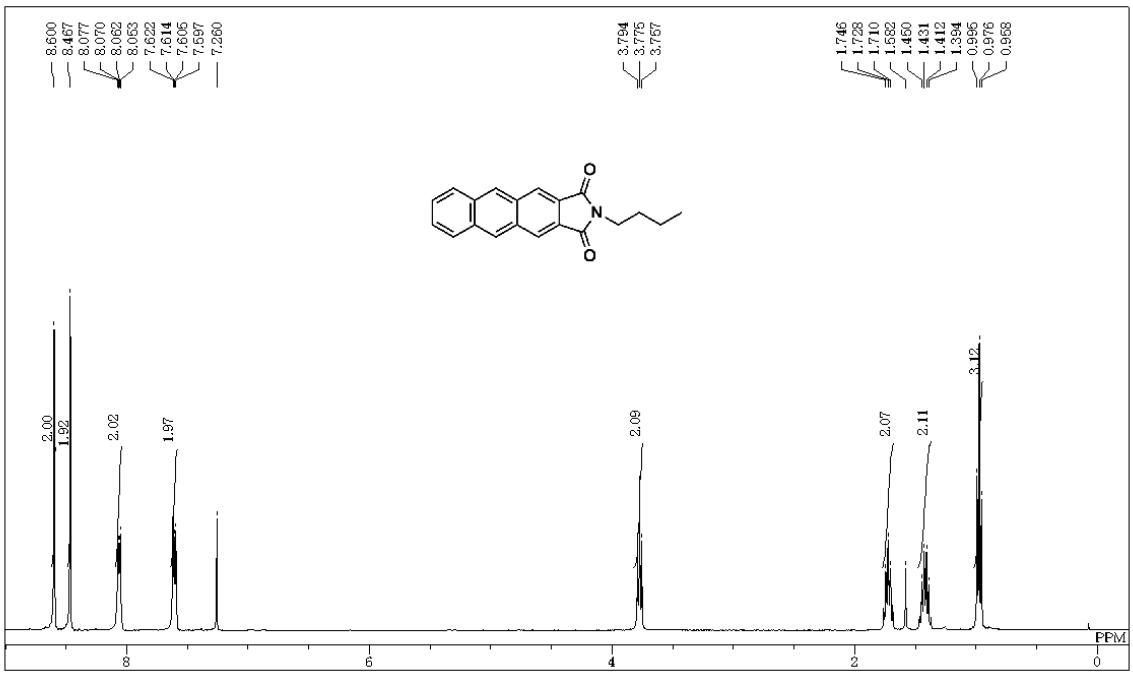

Figure S32. ^{1}H NMR spectrum of **2** in $CDCl_3$.

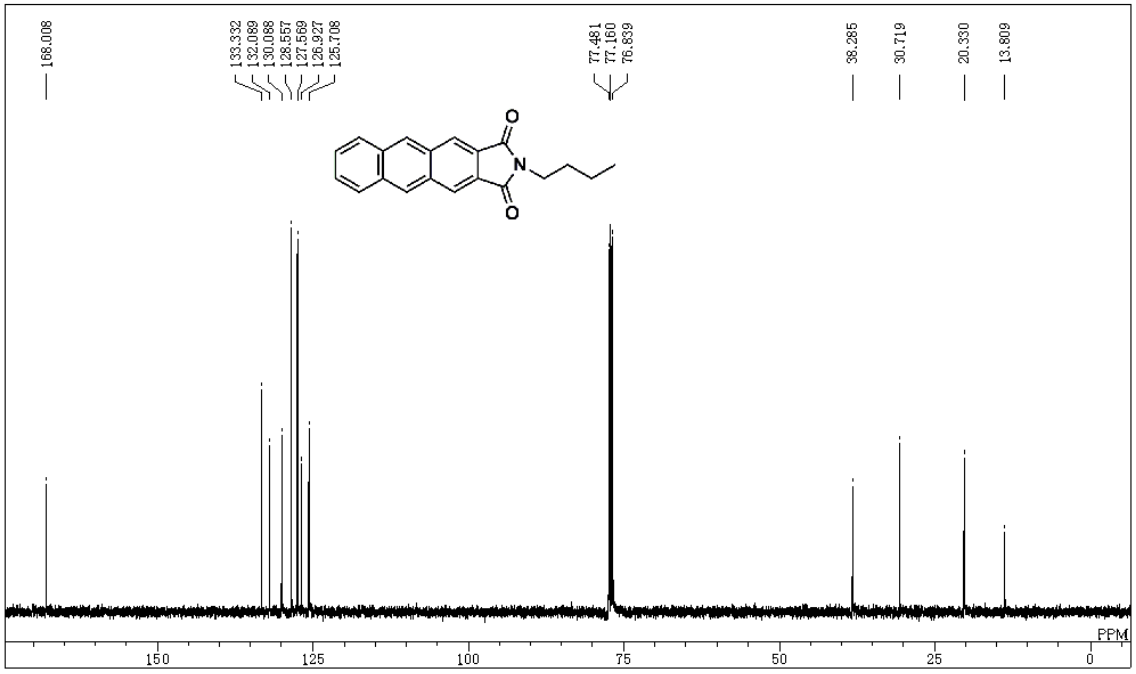

Figure S33. ^{13}C NMR spectrum of **2** in $CDCl_3$.